THESIS

CALIBRATION OF AN IRRADIATION FACILITY

Submitted by

Rion Marcinko

Department of Environmental and Radiological Health Sciences

In partial fulfillment of the requirements

For the Degree of Master of Science

Colorado State University

Fort Collins, Colorado

Spring 2017

Master's Committee:

Advisor: Thomas Johnson

Alexander Brandl
Colleen Duncan

ABSTRACT

CALIBRATION OF AN IRRADIATION FACILITY

The objective of this research is to provide accurate reliable data for use in an irradiation facility and present findings in a manner useful to operators. The intended use of the irradiator and irradiator protocols dictate a need for a well-known administered dose. Dose rates from two independent methods were investigated at multiple distances away from the source. First, the irradiation platforms were examined for “hot spots” using Gafchromic © film to provide a qualitative estimate of the dose distribution. A quantitative assessment of doses was then performed using Fricke dosimetry (a primary standard). Finally, MCNP modeling was used to simulate irradiation at the various measured points and intermediate points in the radiation field. The results were used to provide dose rates within the radiation field for future researchers, and demonstrated how precision and accuracy vary using theoretical (MCNP) and measurement methodology. MCNP simulation matched the Fricke measurements within 10% for the first two positions explored, then diverged upon further movement from the source.

ACKNOWLEDGMENTS

A special thanks to Thomas Johnson for laboratory instruction on Fricke chemistry. Also, helping to obtain materials and proofing/editing this thesis. Instruction from Alex Brandl on MCNP software, radiation physics, and results troubleshooting were crucial in completion of this project. MCNP code and simulations created were a direct result of significant contributions from Justin Bell, Jenelle Mann, and Andrew Owens. CSU irradiator instruction, operations, and certification were from Radiation Safety Officer, Jim Abraham.

TABLE OF CONTENTS

LIST OF TABLES

LIST OF FIGURES

CHAPTER 1 - INTRODUCTION

Irradiators typically use gamma emitting radioactive sources to deliver high radiation doses to a variety of media. Some uses include the study of radiation effects, sterilization of medical equipment, preservation of food, calibration of radiation dosimetry equipment, and sterilization of insects (Irradiators, 2016). Common sealed sources used in irradiators include Cesium-137 and Cobalt-60. Source activity and facility designs are usually well-documented making irradiators very useful and reliable.

Colorado State University (CSU) has seven irradiators of differing designs that are utilized for research and sterilization. Accurate dose rate measurements are necessary for experiments spanning several departments and topics of study. Irradiators are surveyed periodically to ensure proper operation as well as the safety of those who operate the facility by the University's Radiation Control Office (RCO) (Radiation Control Manual, 2016); but to the knowledge of both operators and staff, no comprehensive evaluation of the dose rates have been performed in recent years. No authoritative record of the dose rates produced by the irradiator were available, and an objective of this project was to produce useful, accurate, information on dose rates at various locations.

Cesium-137 is a radioactive element that decays by the emission of a beta particle. 94.6% of these decays result in Barium-137m, a metastable element that releases a 0.662 MeV gamma, for an overall emission fraction of 85.1% per decay to stable Ba-137. Cs-137 is assumed to be in secular equilibrium with Ba-137m. The complete decay scheme is in Figure 1.

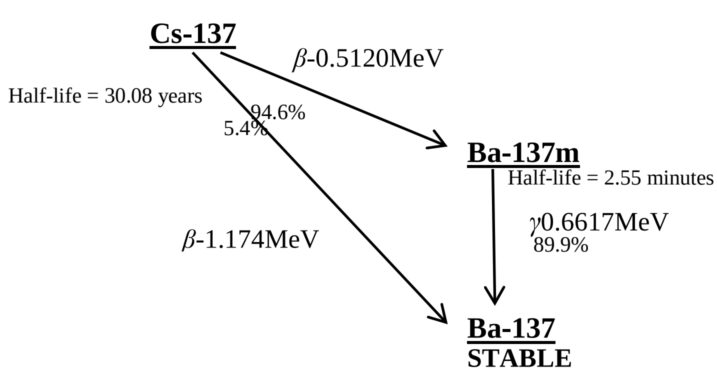

Figure 1: Decay Scheme of Cs-137
Note that the 0.662 MeV gamma ray appears in 89.9% of decays from Cs-137 to Ba-137 (stable)

A thorough calibration of CSU's J.L. Shepherd irradiators has not been performed to the knowledge of any faculty and staff, although irradiator calibration has been accomplished by other organizations in the past. One type of calibration performed by the National Institute of Standards and Technology (NIST) used traceable sources and air kerma values (Minniti 2007). Equivalent dose was measured at different distances using multiple primary standard air ionization chambers in 2006. Other research includes dose mapping with particle simulation software combined with benchmarking using various chemical dosimetry of an Ir-136 irradiator, and using Fricke dosimetry (which will be described later) to measure dose rates from a Co-60 pool irradiator (Sohrabpour, 2002a; Sohrabpour, 2002b; Wang, 2008). Each of the aforementioned irradiator types are used for entirely different purposes than those at Colorado State University; however, similar principles were utilized. Additionally, no documentation of dose rates at any point on the J.L Shepherd irradiator shelf was available. Operators had been using inverse square law relationships and assuming ideal isotropic emission conditions exist in order to ascertain dose rates.

Exact dose assessments for this type of irradiator are difficult both in the conduct of physical measurement as well as due to the fact that machine details are not readily available due to security concerns. The dose administered by the irradiator is integral to the findings and research of media exposed. The objective of this research is to provide accurate reliable data for use in future irradiations and present findings in a manner useful to operators. Two separate independent methods measured dose rates at multiple distances away from the facility source. Each of measurement methods will agree within 10%, or the limitations of the dosimetry.

CHAPTER 2 - MATERIALS AND METHODS

The J.L. Shepherd Model 81-14 irradiator (J.L. Shepherd, San Fernando, CA) is located in Room 004 of the Molecular and Radiological Biosciences (MRB) building and has been in use for nearly four decades. The 81-14 model irradiator features an open beam configuration that is collimated and directed vertically towards a moveable wooden shelf below. A Cesium-137 “pill” source, surrounded by thin encapsulating metal, is moved between a shielded and exposed position horizontally. Shown in Figure 2 below, the irradiator is comprised of two lead cylinders. The smaller left cylinder contains a spring a piston assembly; compressed air is used to overcome the spring and move the source located in the larger right cylinder to the middle ported area. Following timed completion or operator shutdown, the air pressure is released and the source returns to the shielded position on the right.

Figure 2: MRB Room 004 Irradiator

A collimator and an aluminum tiered attenuator help control the radiation field. The bottom moveable shelf is used to accommodate different sizes of media to be irradiated. The shelf sits on notches in tracks located on four structural supports, which also suspend the rest of the irradiator apparatus. There are no permanently affixed measuring increments provided to estimate the distance of the source relative to shelf position.

Operator safety is paramount in using the Room 004 irradiator. Many interlocks, alarms, and indicators prevent both inadvertent use as well as personnel exposure. Controls are located outside of the locked facility room and are only accessible by qualified personnel. To ensure the security of irradiator geometries, plans and source information are normally controlled. Access to specific design information is strictly limited, and can only be viewed by permission. Therefore, no specific information on the irradiator can be provided in this document. Information about the irradiator model and source is located in Table 1.

Table 1: Room 004 Irradiator Information

Manufacturer	Model	Source Activity	Current Calculated Activity
J.L. Shepherd	81-14	222 TBq (November 1, 1976)	90.16 TBq (December 2, 2015)

Due to restrictions on the use of schematics, measurements of the external geometries were performed and documented but are not included here (available upon request). J.L. Shepherd provided some internal dimensions for this assessment. The information gathered enhanced the ability to closely model the irradiator and calculate inverse square law relationships, but also revealed a few inconsistencies in the design. The first was that the collimator is not directly centered on the shelf below. Instead, it is off center in the northeast direction viewed from the overhead in Figure 3. It is important to note that the shelf below sits on top of pegs in the irradiators structure and is moveable. For the purposes of this experiment, the shelf was maintained in alignment to a support between the steel beams.

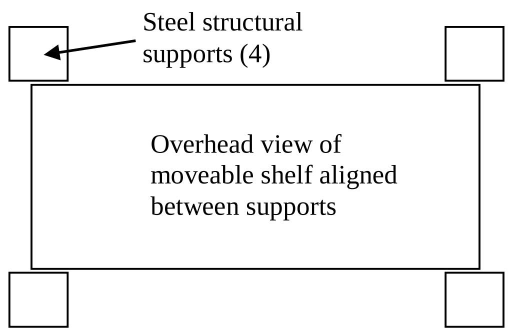

Figure 3: Shelf Alignment between Structural Supports

Gafchromic © film was used to establish a baseline estimate of dose rates at varying shelf positions. The film was developed by International Specialty Products (Ashland Inc., Covington, KY) in 2008 and utilizes a laminated proprietary layer, which darkens to a shade dependent on dose. After exposure, no developing processes are needed, and the film can either be photographed or scanned (“Gafchromic EBT2 and EBT3,” 2014; “Efficient Protocols,” 2016). All Gafchromic EBT3 film was manufactured by Ashland Inc., Lot # 08251503, Exp. August, 2017. To ensure quality during shipping a Temperature History Indicator Card was included in each package shown in Figure 24. All film used maintained a proper temperature history. For the purposes of calibration, Gafchromic film was used to qualitatively ascertain if areas have irregular dose rates.

After the size and shape of the radiation field was determined, a precise measurement of the dose rates on each shelf was performed using Fricke dosimetry. Fricke solution is a mixture of Ammonium Sulfate [$(NH_4)_2FE(SO_4)_2$], Sodium Chloride [NaCl], and diluted Sulfuric Acid [H_2SO_4]. It is the most widely used chemical dosimetry system. Irradiation of this mixture will oxidize ferrous Fe^{2+} ions into ferric Fe^{3+} ions as shown in the five simplified reactions below (Attix, 1966, p.186).

$$H + O_2 \rightarrow HO_2 \ (1)$$

$$Fe^{++} + HO_2 \rightarrow Fe^{3+} + HO_2^- \ (2)$$

$$HO_2^- + H^+ \rightarrow H_2O_2 \ (3)$$

$$Fe^{++} + H_2O_2 \rightarrow Fe^{3+} + OH + OH^- \ (4)$$

$$Fe^{++} + OH \rightarrow Fe^{3+} + OH^- \ (5)$$

Hydroperoxy (HO_2) formed upon exposure to gamma radiation will oxidize three ferrous ions. Each reaction happens quickly (in microseconds), except for reaction 4, which has a half-life of 14 seconds. Following gamma exposure, no corollary reactions are present (Attix, 1966, p.186). The oxidized Fe^{3+} ions exhibit strong absorption peaks at a nonvisible spectrum wavelength of approximately 304 nm, whereas Fe^{2+} ions (un-reacted) do not show any absorbance (Podgorsak, 2005). The absorbance value given by a spectrophotometer is translated into dose after standardizing for temperature and accounting for certain constants and ferrous ion yields, which will be described later.

Use of the chemical dosimetry as a reliable science is also commensurate for irradiator analysis. “Fricke Dosimetry is an established primary reference standard and used for standardization of Category-I irradiators” (Vandana 2011). According to the International Atomic Energy Agency (IAEA), CSU’s JL Shepherd irradiator is classified as a Category-I type, making Fricke an excellent tool for dosimetry analysis and calibration (Al-Mughrabi, 2007).

Gafchromic EBT3 film was specifically chosen as the particular type best suited for this experiment. The targeted applications for Gafchromic film are in hospital radiotherapy devices. It has a wide range of exposure compared to similar films and the highest degree of indoor light resistance. Previous designs would darken in only a few hours of exposure to synthetic light. The film contains two polyester layers that provide water resistance and protection of the proprietary active layer. Temperature is also not a factor in the use of the film as it can withstand temperatures of up to 70°C ("Efficient Protocols," 2016).

The methodology for Fricke placement was first determined by the irradiation of GafchromicEBT3 film at four shelving heights, measured from the bottom of the aluminum attenuator plate below the collimator shown in Figure 4. Shelf distances displayed in Table 2 below were used. Due to the mechanics designed to raise and lower the moveable shelf, only certain distances were permissible. Each height was changed by approximately 10 cm to provide a near linear comparison in data. Irradiation times were chosen to safely fall within the range required for the film at 0.02-10 Gy. Currently, there was no accurate documentation to closely determine any given exposure and thus, estimate calculations were completed.

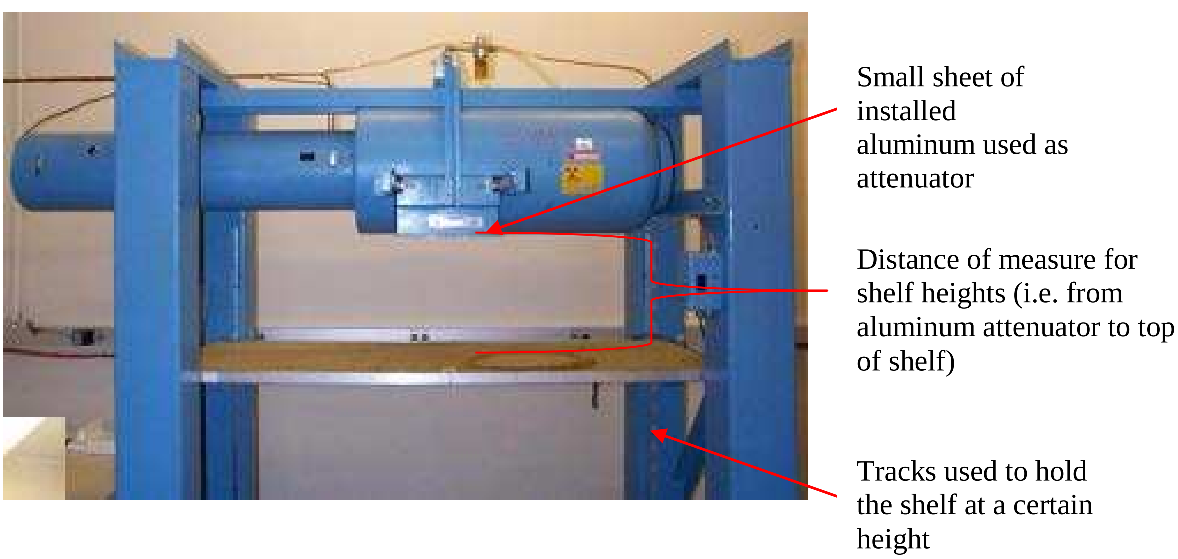

Figure 4: MRB 004 Irradiator Diagram

Table 2: Shelf Height Determination

Shelf	Distance from Attenuator	Gafchromic Exposure Time	Reasoning
1	14 cm	8 min	Most common shelf height; used in the irradiation of caged laboratory mice
2	25 cm	9 min	Distance for linear comparison
3	34 cm	12 min	
4	41.75 cm	16 min	Far enough to accommodate large items, calculated distance of irradiation field to the edge of the shelf

Shelf dimensions of 48.895 cm (19.25 in) by 141.605 cm (55.75 in) were measured with standard units in the placement of Gafchromic sheets. Fourteen film sheets per shelf were used in two distinct rows, and each sheet cut from its original standard unit dimensions of 20.32 cm (8 in) by approximately 25.4 cm (10 in) in height. Equal modifications were made to both sheets to maintain proper centerline. Total overlap upon placement was less than one cm on each side of the shelf. Following exposure, each piece of film was labeled in a manner to ensure proper interpretation of the dose field. The top row was labeled in the upper left-hand corner, the bottom row labeled in the bottom left-hand corner. During handling, nitrile gloves were worn to eliminate fingerprinting, which can cause false shadowing on film. The film was then scanned and photographs properly aligned in Figures 20-23. Between irradiation and scanning, film exposure to light was minimized during storage.

The image created in the Gafchromic film displays a consistent expanding radiation field as the distance is increased. The irradiated film does show a slight off centered field towards the right side which is due to aforementioned flaws in the irradiator design. From each film's shading, Fricke dosimeter placement was determined by placing plotting paper directly on the surface of the shelf analogous to the exposed area. Due to the standard size of each of Gafchromic film sheet, precise measurements could be made using sheet dimensions to determine the changing dose rate away from the irradiator's collimator. For example, if the exposure field started on the middle of the third sheet (from left to right), dosimetry could be placed at around 50.8 cm (20 in) from the edge of the shelf. More importance was given to determine dose distribution in the horizontal direction on the shelf than the vertical. Therefore, a total of four rows of Fricke dosimeters were chosen, and a map created. Each of the proposed Fricke dosimeter locations were staggered such that a proper dose measurement every 5 cm (2 in) increment was completed. Each dosimeter location was labeled in terms of its zone associated with shelf position, as well as dosimeter number. Dosimeter positioning is shown in Figure 33, with the total number of scintillation vials or dosimeters that was used (vials to be discussed below).

Fricke preparation was in accordance with the American Society for Testing and Materials (ASTM) E 1026-13(ASTM Standards, 2015). Chemical information, amount, and combination to create 1 liter of solution are shown in Table 3. Sulfuric acid was measured by a Mettler PM300 scale (Mettler-Toledo Inc, Broomfield, CO) into a 100 mL graduated cylinder. The 41 g of required acid is equivalent to approximately 23 mL. The sulfuric acid (Mallinchridt, St. Louis, MO) was diluted into Liquid Chromatography Mass Spectrometry (LCMS) water (OmniSolve Inc., McLean, VA) and subsequent chemicals were mixed in. LCMS water was chosen due to its extreme purity compared to other water types. ASTM E 1026-13 requires a minimum of double distilled water or purer. Ferrous Ammonium Sulfate and Sodium Chloride were measured by a Mettler AE200 scale. Personal Protective Equipment (PPE) included nitrile gloves, safety glasses, and a laboratory jacket along with full coverage of legs and feet.

Table 3: Fricke Chemical Information

Chemical Name	Amount (g/liter)	Manufacturer	Lot #
Ferrous Ammonium Sulfate $[(NH_4)_2FE(SO_4)_2]$	0.392 g	Aldrich Chemistry	MKBR8854V
Sodium Chloride [NaCl]	0.058 g	Mallinckrodt	G24629
Sulfuric Acid $[H_2SO_4]$	41 g (23 mL)	Mallinckrodt	2876B03003
Pure Water (LCMS) $[H_2O]$	977 mL	EMD Millpore Corp	55152

Wheaton Scientific Liquid Scintillation Vials were chosen to contain the Fricke solution during irradiation. Wheaton Scientific plastic vials (Wheaton Industries Inc., Millville, NJ) have a density of 0.87 g/cm^3 (K. Dare personal communication, October 23, 2015). Plastic was chosen over glass as to contain the Fricke solution during irradiation of the medium due to its low density and to minimize gamma ray attenuation. Each vial was rinsed three times with 5 mL of Fricke solution and filled with a final 5 mL as specified by the ASTM procedure. Five mL was chosen such that the resulting dose rate would translate closely to the level of the shelf, and multiple readings of sample solution could be analyzed, if needed. The solution in each capped vial measured about 1.5 cm in height above the bottom of the vial, measured at the bottom of the meniscus.

Fricke requires a dose range of 20-400 Gy. Dose results from the first shelf were used in determining the irradiation times as the shelf was moved further away from the source. After irradiation, the Fricke solution was transferred to cuvettes manufactured by VWR (Radnor, PA) and inserted into a spectrophotometer which interrogated the sample at a wavelength of 303 nm in order to calculate absorbance. Temperatures at the time of irradiation and during spectrophotometer readings were standardized to 25°C, and a dose was then calculated based on absorbance. Sample time and temperature are displayed in Table 4. In each case, an additional vial with Fricke solution was maintained as a blank.

Table 4: Fricke Irradiation Times Per Shelf Position

Shelf	Irradiation Time	Temp Irradiated	Temp Analyzed
1	240 min	17°C	23.1°C
2	480 min	17°C	23.3°C
3	960 min	17°C	25.8°C
4	1800 min	17°C	21.8°C

The spectrophotometer used was a Beckman DU 530 (Beckman Coulter Inc., Brea, CA) in Figure 27. A cuvette blank, separate from the blank dosimeter in each shelf experiment, of LCMS water was established prior and between each Fricke dosimeter reading to ensure no drift occurred between samples. The maximum drift observed throughout each reading was 0.001 absorbance. Samples were read twice to ensure accuracy of the analysis. Once irradiated and analyzed, used vials were discarded. All used Fricke was treated as Hazmat, and disposed of accordingly. Absorbance was converted into dose by the following equation found in the Fricke ASTM.

$$D_f = \frac{\Delta A[1+0.0069\,(25-T_{meas})][1+0.0012\,(25-T_{irrad})]}{(\varepsilon_{25}\cdot G_{25}\cdot \rho \cdot d)} \quad (6)$$

Where, ΔA represents the change in absorbance between the blank, accounting for oxidation. The numerator converts constants and accounts for a change in temperature when irradiated and measured. ε and *G* values represent ferrous ion yield standards at 25°C. The value ρ represents a given density of the liquid when mixed properly at 25°C. The value *d* is the optical path length, or distance through the cuvette (ASTM Standards, 2015). Typical oxidation of a Fricke sample is about 2×10^{-6}M/day at 25°C, meaning a batch of Fricke could be stored for extended periods (though it is recommended to produce a new batch for occasional use). If the spectrophotometer absorbance value of the blank sample is high, it either means that the sample is old or more likely there are a high number of impurities and the solution may need to be discarded (Attix, 1966, p.187-188).

Utilizing Fricke results, contoured “heat maps” of the radiation dose rates were created using Origin graphic software (OriginLab, Northampton, MA) that allow a direct visual correlation between dose measured and position on each shelf. The Origin maps can be printed and used in direct placement on the irradiator shelf for future applications of the CSU irradiator.

Measurements of the Room 004 facility were completed using a Snap-on TMPA12 tape measure (Snap-on Tools International, LLC, Kenosha, WI). A tape measure in inches was used due to the U.S. standard measuring system used by J.L. Shepherd in design and manufacturing. Measurements were converted into centimeters, which are required in particle simulation software. Using knowledge of the dimensions inside the collimator as well as the source, the inner open volume of the machine was calculated. Pictured in Figure 5 are the cross sectional cutaways of the model. The inner volume dimensions were unknown and created at a radius that would not interfere with the photon path from the source, through the collimator, and to the shelf below. Due to the small fraction of dose shielded by the plastic vials, each vial was not included in the coding. Instead, point detectors (F5 tallies) of relative size were placed in the exact positions shown in Figure 9.

Finally, to compare the Fricke results, the Room 004 irradiator was modeled using Monte Carlo N-Particle 6 (MCNP) software (MCNP6, LANL, Los Alamos, NM). MCNP is a well-established software program created from the Los Alamos National Laboratory (LANL) that is used to simulate over 37 different particle types in three-dimensional space. Randomized statistical probabilities of every particle's travel are calculated and processed in the defined areas. Uses include modeling for shielding, dosimetry, detector response, and many others (Goorley 2013). The coding process includes geometric, source, and material/density specifications. Measurements and material estimates were generated as well as tally specifications directly specified from the Figure 33 dosimeter map. Tallies are the measurement of the particle flux through the area specified, and can be segmented based on a range of energies. Tally dimensions were in the shape of a sphere with a radius similar to the amount Fricke solution inside each dosimeter. Point detector tallies were specifically used with an output in pGy per starting particle. Results are converted into conventional dose rate units by the following equation. Starting particle is converted to particles per second or decays per second by an activity input from the user.

$$\dot{DR}\left(\frac{\text{Gy}}{\text{hr}}\right) = \left(\frac{\text{pGy}}{\text{Starting particle}}\right)\left(\frac{\text{Gy}}{\text{pGy}}\right)\left(\frac{\text{Particles}}{\text{sec}}\right)\left(\frac{\text{sec}}{\text{hr}}\right) \quad (7)$$

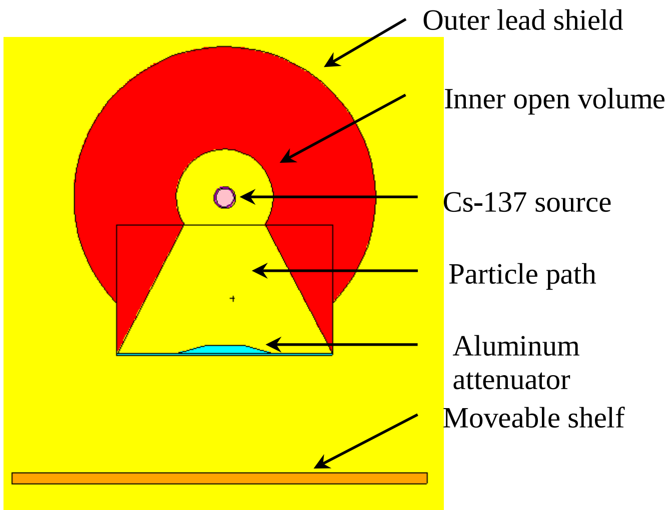

Side cutout view

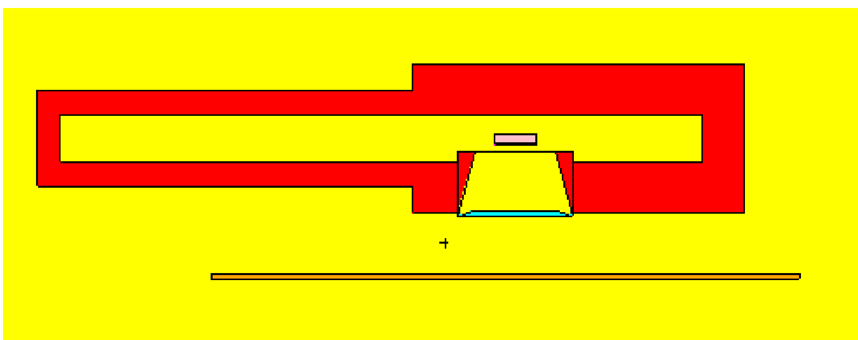

Front cutout view

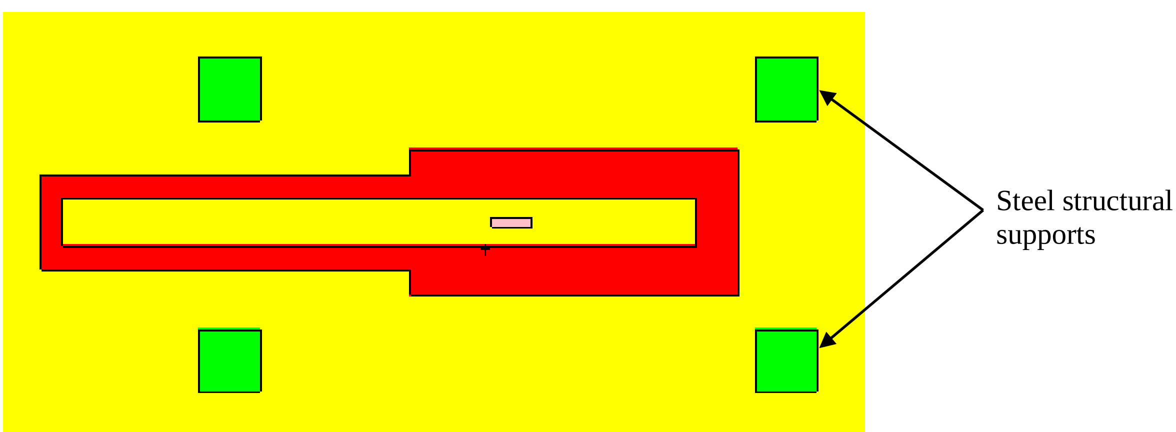

Overhead view

Figure 5: MCNP modeling of J.L. Shepherd irradiator Model 81-14

CHAPTER 3 - RESULTS

With respect to CSU's J.L. Shepherd Model 81-14 irradiator, Fricke dosimetry and Origin software proved that an irregular beam geometry was present on Shelf 1 at 26 cm from the source in Figure 6. Shelves 2-4 in Figures 7-9 showed a normal distribution while maintaining a logarithmic scale of dose on the x-axis. Inverse square comparison of averaged dosimeters 19-21; 31-33 for Fricke dosimetry closely matched a normal distribution compared to MCNP in Figures 10-11.

Complementary experiments with Fricke dosimetry and MCNP modeling confirmed overall beam patterns with higher MCNP peak dose rates in Figures 16-19, and did not reproduce the irregularity on Shelf 1. Plotted results confirmed a near linear ($y=x$) comparison between both methods with identical dosimeter locations in Figures 12-15. Both methods agreed within 10% on Shelf 1 and 2 with the exception of the irregularity of the first row of dosimetry on Shelf 1 as seen in Figures 12 and 16. Shelves 3-4 displayed diverging peak dose rates as dosimetry was moved further from the source. A two-tailed Z test performed on dose rate data from each method and shelf showed a statistical difference in means. Z test value results validate each method as independent and sufficient to use in determining calibration. Source activity calculated from averaged dosimeters 19-21; 31-33 using the point source equation differed by over 70% of the posted activity on the irradiator, accounting for decay.

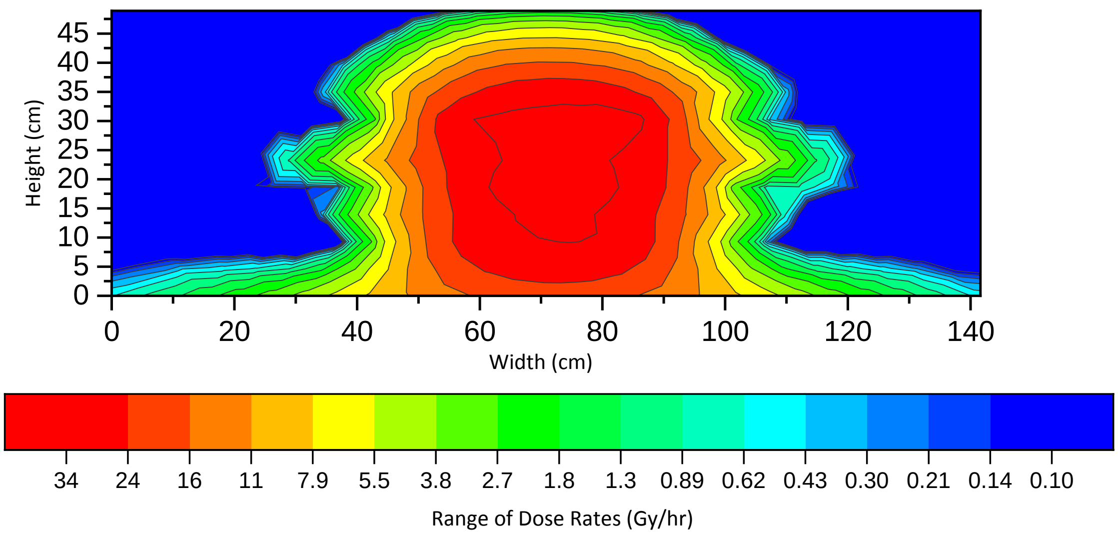

Figure 6: Fricke Origin Heat Map for Shelf 1 (26 cm from Source)

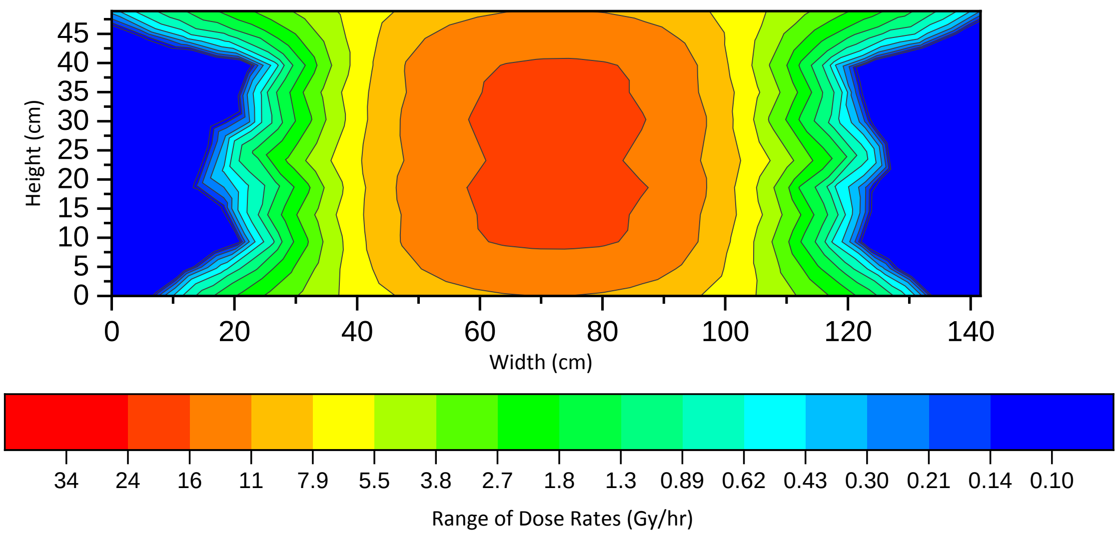

Figure 7: Fricke Origin Heat Map for Shelf 2 (37 cm from Source)

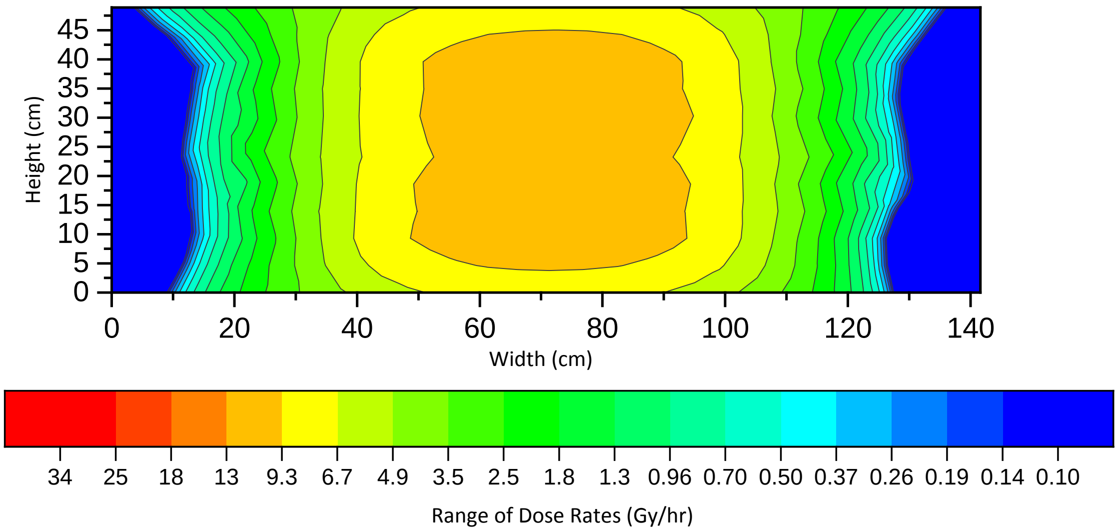

Figure 8: Fricke Origin Heat Map for Shelf 3 (46 cm from Source)

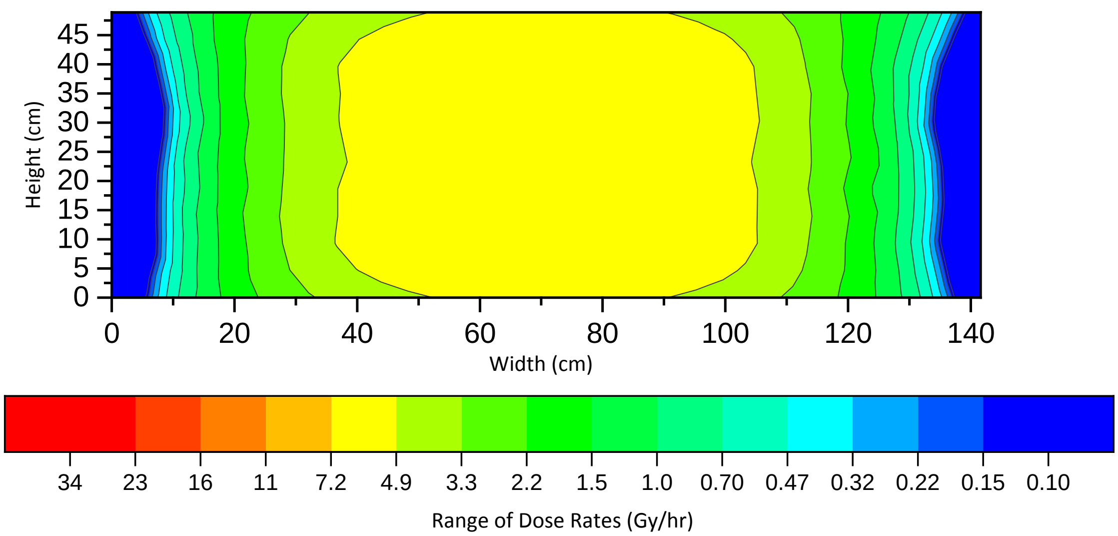

Figure 9: Fricke Origin Heat Map for Shelf 4(53.75 cm from Source)

Table 5: Fricke Dose Rates per Dosimeter Number and Shelf Height

	Shelf1	Shelf1(2)	Shelf2	Shelf3	Shelf4
#	Gy/hr	Gy/hr	Gy/hr	Gy/hr	Gy/hr
1					0.514442
2			0.035363	0.79949	1.914869
3	0.662818	0.42494	1.096265	3.319624	3.763051
4	1.230948	1.274819	6.153232	6.708768	5.354012
5	6.722869	7.365621	13.22591	9.315802	6.239996
6	15.05544	14.3063	15.66599	10.11529	6.40195
7	14.29793	16.57265	16.37326	10.30648	6.544851
8	11.36259	13.45642	16.16107	10.27171	6.478164
9	6.438804	7.932207	14.35754	9.698167	6.363844
10	1.136259	2.124698	7.07268	7.038992	5.430226
11	0.56813	0.566586	1.803533	3.441285	3.582044
12			0.141454	1.147095	1.743388
13					0.581129
14				0.504027	1.047938
15			0.459724	1.998726	2.762746
16	0.946883	0.354116	3.783884	5.196688	4.639509
17	5.586609	5.949155	10.53829	8.290369	5.954195
18	27.93305	26.98367	15.91353	10.27171	6.440057
19	33.70903	31.23306	17.39879	10.6367	6.668698
20	34.84529	29.95825	17.89388	11.00168	6.649645
21	31.62589	29.25001	16.90371	10.5498	6.544851
22	10.60509	8.42797	12.16501	9.194141	6.325737
23	0.662818	0.708233	4.066791	5.387871	4.782409
24			0.742631	2.085627	2.791327
25				0.451886	1.133679
26					0.485862
27			0.459724	0.869011	1.848182
28	0.284065	0.495763	1.697443	3.493426	3.829738
29	1.230948	1.416465	7.143407	6.969471	5.392119
30	16.28639	16.99759	14.21609	9.715547	6.421004
31	31.72058	31.09142	16.93907	10.42814	6.554378
32	34.7506	33.64106	17.64634	10.75836	6.640118
33	33.80372	32.93282	17.39879	10.61932	6.706805
34	22.06237	20.75122	15.5599	10.13267	6.563904
35	2.935337	1.912228	8.098219	7.386597	5.601707
36	0.662818	0.495763	1.944987	3.701989	3.734471
37			0.247544	1.094954	1.838655
38					0.619236
39				0.434506	1.143205
40			0.495088	2.016106	2.743693
41	0.56813	0.566586	3.854611	5.196688	4.696669
42	4.829103	5.665862	10.50293	8.759635	5.992302
43	25.37646	25.49638	15.20626	9.993631	6.421004
44	29.9215	29.25001	16.30253	10.41076	6.525798
45	31.43651	29.67495	16.37326	10.41076	6.582958
46	27.93305	26.70037	15.70135	10.21957	6.506744
47	7.859128	7.365621	11.06874	8.881296	6.268576
48	1.136259	0.779056	4.066791	5.248829	4.639509
49			0.671905	2.068247	2.705586
50					1.181312

Table 6: MCNP Tally Results pGy Per Starting Particle and Gy/hr with Percent Relative Error

		Shelf1			Shelf2			Shelf3			Shelf4		
#	Tally	pGy/SP	Gy/hr	Error	pGy/SP	Gy/hr	Error	pGy/SP	Gy/hr	Error	pGy/SP	Gy/hr	Error
1	5										5.44E-07	0.110	0.004
2	15				1.32E-06	0.266	0.038	8.00E-07	0.161	0.0062	7.65E-07	0.154	0.004
3	25	1.38E-06	0.279	0.008	7.98E-06	1.606	0.005	1.63E-05	3.272	0.0028	1.87E-05	3.758	0.002
4	35	8.23E-06	1.655	0.009	3.10E-05	6.233	0.003	3.40E-05	6.844	0.0017	3.18E-05	6.402	0.002
5	45	6.99E-05	14.058	0.002	6.95E-05	13.986	0.001	5.26E-05	10.583	0.0012	4.14E-05	8.332	0.002
6	55	1.30E-04	26.223	0.001	8.45E-05	16.998	0.002	6.06E-05	12.196	0.0014	4.64E-05	9.330	0.002
7	65	1.48E-04	29.812	0.001	9.17E-05	18.453	0.001	6.43E-05	12.938	0.0012	4.87E-05	9.795	0.001
8	75	1.41E-04	28.407	0.001	8.88E-05	17.867	0.001	6.28E-05	12.633	0.0012	4.78E-05	9.614	0.001
9	85	1.13E-04	22.681	0.002	7.68E-05	15.464	0.001	5.66E-05	11.391	0.0018	4.38E-05	8.823	0.002
10	95	1.60E-05	3.230	0.004	3.89E-05	7.832	0.002	3.93E-05	7.916	0.0017	3.55E-05	7.147	0.002
11	105	2.06E-06	0.415	0.007	1.61E-05	3.246	0.004	2.31E-05	4.641	0.0022	2.41E-05	4.840	0.003
12	115				2.38E-06	0.480	0.009	9.29E-06	1.869	0.0044	1.29E-05	2.599	0.002
13	125										5.54E-06	1.115	0.005
14	135							1.14E-06	0.228	0.0522	3.36E-06	0.676	0.006
15	145				1.38E-06	0.277	0.008	6.17E-06	1.241	0.0054	1.01E-05	2.031	0.006
16	155	1.81E-06	0.365	0.008	1.13E-05	2.280	0.006	1.85E-05	3.731	0.0033	2.02E-05	4.062	0.002
17	165	1.87E-05	3.762	0.007	3.91E-05	7.865	0.002	3.85E-05	7.754	0.0022	3.45E-05	6.946	0.001
18	175	1.15E-04	23.106	0.001	7.10E-05	14.298	0.001	5.16E-05	10.393	0.0015	4.05E-05	8.160	0.002
19	185	1.50E-04	30.274	0.003	8.48E-05	17.074	0.002	5.88E-05	11.825	0.0015	4.49E-05	9.043	0.002
20	195	1.58E-04	31.743	0.001	8.77E-05	17.648	0.002	6.02E-05	12.119	0.0016	4.57E-05	9.198	0.001
21	205	1.29E-04	25.941	0.002	7.70E-05	15.493	0.002	5.49E-05	11.046	0.0012	4.28E-05	8.606	0.002
22	215	4.87E-05	9.799	0.003	5.64E-05	11.358	0.002	4.72E-05	9.495	0.0017	3.75E-05	7.548	0.002
23	225	2.63E-06	0.528	0.007	2.05E-05	4.127	0.003	2.56E-05	5.149	0.0023	2.56E-05	5.157	0.002
24	235				2.61E-06	0.525	0.014	1.05E-05	2.103	0.0040	1.36E-05	2.731	0.002
25	245							1.91E-06	0.385	0.0073	5.75E-06	1.157	0.006
26	255										3.06E-06	0.616	0.010
27	265				1.29E-06	0.260	0.029	6.72E-07	0.135	0.0058	8.88E-06	1.786	0.003
28	275	1.57E-06	0.316	0.016	7.24E-06	1.458	0.004	1.53E-05	3.083	0.0030	1.76E-05	3.552	0.003
29	285	6.25E-06	1.259	0.008	2.95E-05	5.939	0.003	3.20E-05	6.431	0.0019	3.02E-05	6.067	0.001
30	295	7.35E-05	14.795	0.002	6.66E-05	13.408	0.002	4.90E-05	9.863	0.0016	3.88E-05	7.808	0.002
31	305	1.40E-04	28.208	0.001	8.07E-05	16.239	0.001	5.65E-05	11.375	0.0018	4.36E-05	8.778	0.002
32	315	1.64E-04	32.909	0.001	8.89E-05	17.896	0.001	6.06E-05	12.187	0.0013	4.59E-05	9.245	0.002
33	325	1.54E-04	30.983	0.001	8.56E-05	17.227	0.001	5.90E-05	11.870	0.0015	4.50E-05	9.046	0.002
34	335	1.20E-04	24.051	0.002	7.28E-05	14.648	0.002	5.25E-05	10.558	0.0023	4.09E-05	8.232	0.002
35	345	1.51E-05	3.045	0.004	3.71E-05	7.472	0.002	3.73E-05	7.509	0.0022	3.37E-05	6.786	0.001
36	355	2.09E-06	0.421	0.008	1.55E-05	3.112	0.004	2.17E-05	4.370	0.0020	2.28E-05	4.583	0.002
37	365				1.91E-06	0.384	0.010	8.86E-06	1.783	0.0029	1.24E-05	2.490	0.004
38	375										5.28E-06	1.062	0.004
39	385							1.16E-06	0.233	0.0074	3.66E-06	0.737	0.006
40	395				1.48E-06	0.299	0.010	6.58E-06	1.325	0.0050	1.06E-05	2.124	0.003
41	405	1.59E-06	0.320	0.010	1.20E-05	2.408	0.004	1.97E-05	3.961	0.0020	2.15E-05	4.325	0.002
42	415	1.92E-05	3.871	0.007	4.08E-05	8.212	0.002	4.08E-05	8.210	0.0018	3.66E-05	7.363	0.001
43	425	1.07E-04	21.632	0.003	7.48E-05	15.054	0.003	5.59E-05	11.243	0.0014	4.37E-05	8.802	0.001
44	435	1.36E-04	27.400	0.001	8.71E-05	17.538	0.001	6.29E-05	12.651	0.0015	4.80E-05	9.652	0.002
45	445	1.42E-04	28.582	0.001	8.94E-05	17.989	0.001	6.42E-05	12.926	0.0020	4.88E-05	9.811	0.002
46	455	1.21E-04	24.390	0.001	8.03E-05	16.163	0.001	5.92E-05	11.915	0.0015	4.58E-05	9.222	0.001
47	465	4.62E-05	9.304	0.003	5.82E-05	11.704	0.002	5.01E-05	10.091	0.0014	4.02E-05	8.093	0.002
48	475	3.54E-06	0.713	0.012	2.13E-05	4.295	0.003	2.74E-05	5.512	0.0038	2.73E-05	5.493	0.002
49	485				3.35E-06	0.675	0.006	1.10E-05	2.212	0.0029	1.45E-05	2.923	0.004
50	495							2.33E-06	0.470	0.0095	6.03E-06	1.213	0.005

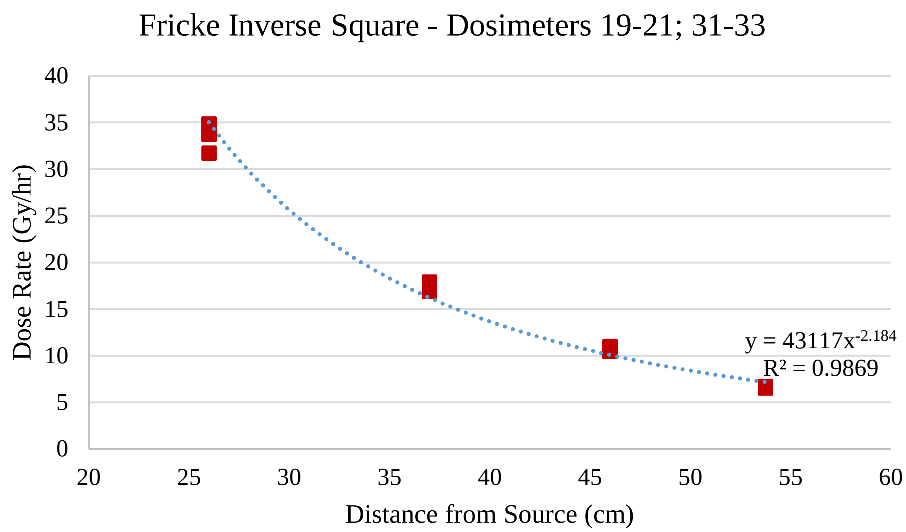

Figure 10: Fricke Inverse Square Graph on All Four Shelves Using Dosimeters 19-21; 31-33 Note that the Fricke graphical value of $x^{-2.18}$ is similar to a perfect inverse square or $y=x^{-2}$

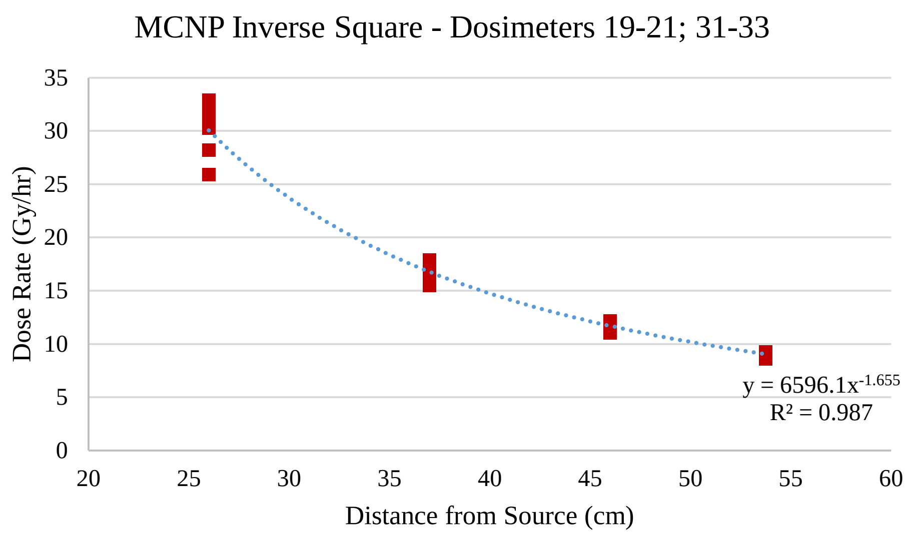

Figure 11: MCNP Inverse Square Graph on All Four Shelves Using Dosimeters 19-21; 31-33 Note that the MCNP graphical value $x^{-1.65}$ further from a perfect inverse square or $y=x^{-2}$ compared to Fricke dosimetry

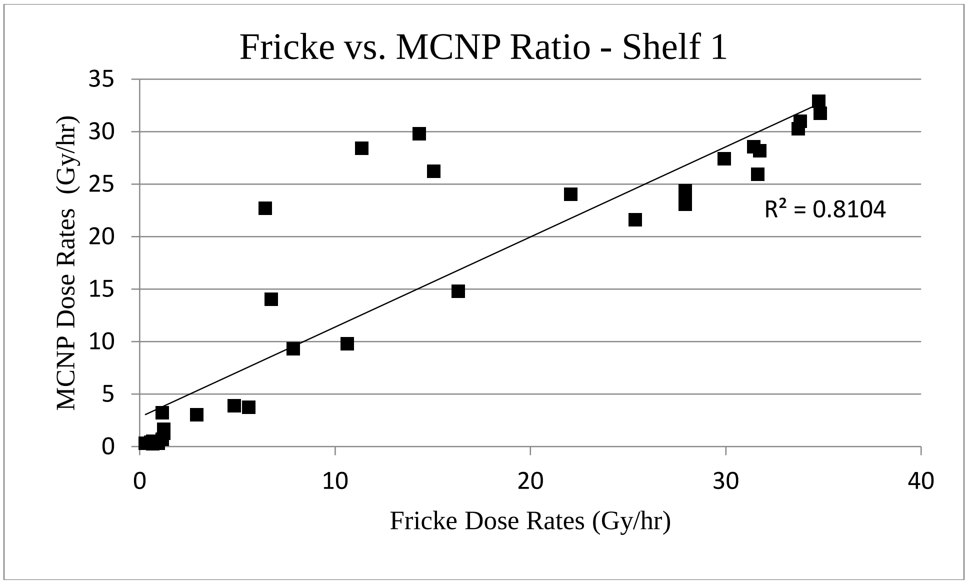

Figure 12: Ratio of Fricke vs. MCNP Dose Rates on Shelf 1 (26 cm from Source)
Note that graph outliers are all the result of inconsistencies found in Fricke dosimeters 3-11 on Shelf 1

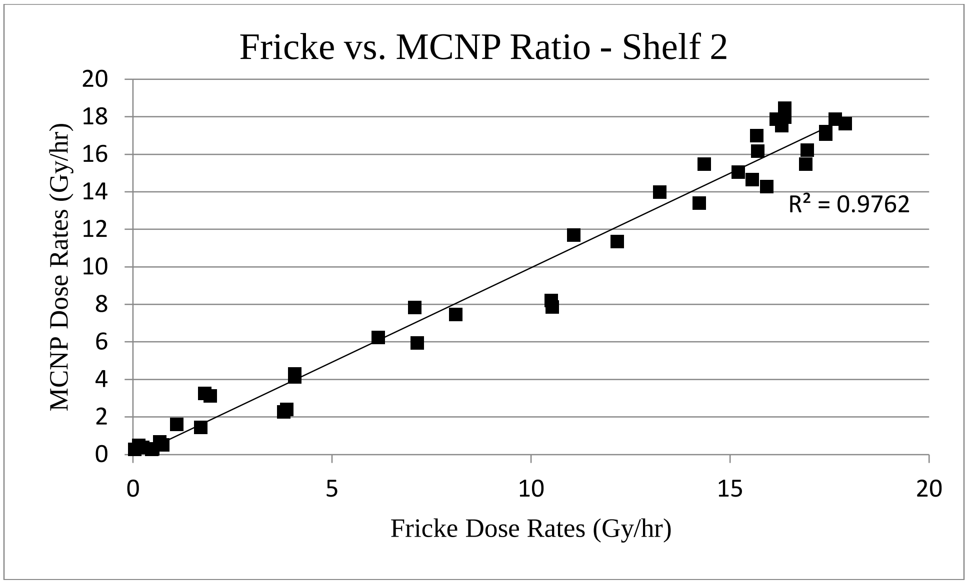

Figure 13: Ratio of Fricke vs. MCNP Dose Rates on Shelf 2 (37 cm from Source)

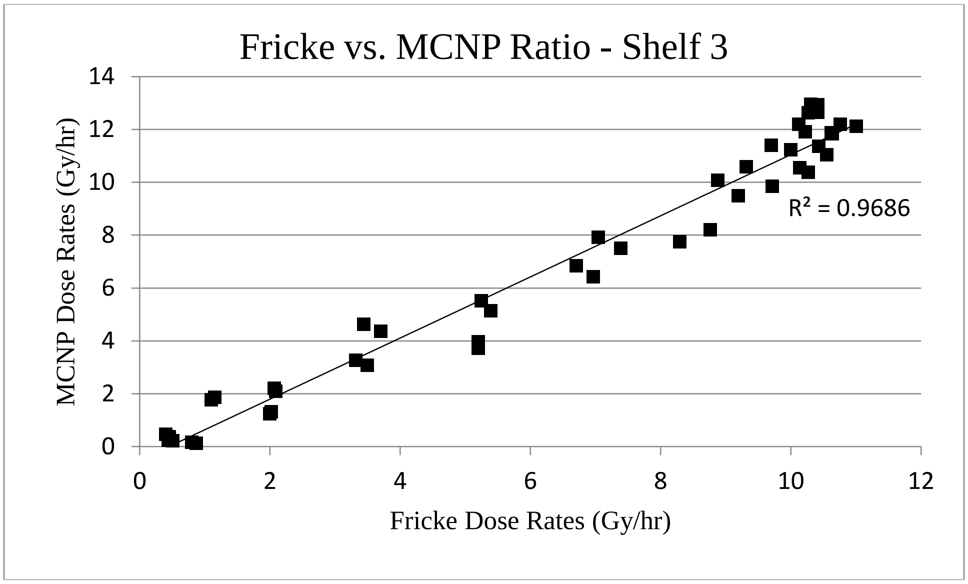

Figure 14: Ratio of Fricke vs. MCNP Dose Rates on Shelf 3 (46 cm from Source)

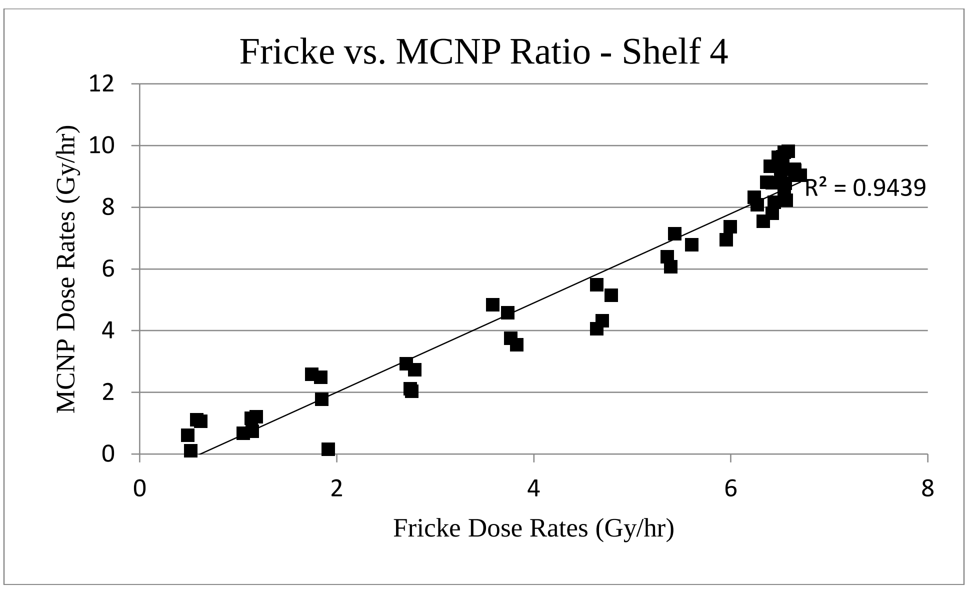

Figure 15: Ratio of Fricke vs. MCNP Dose Rates on Shelf 4 (53.75 cm from Source)

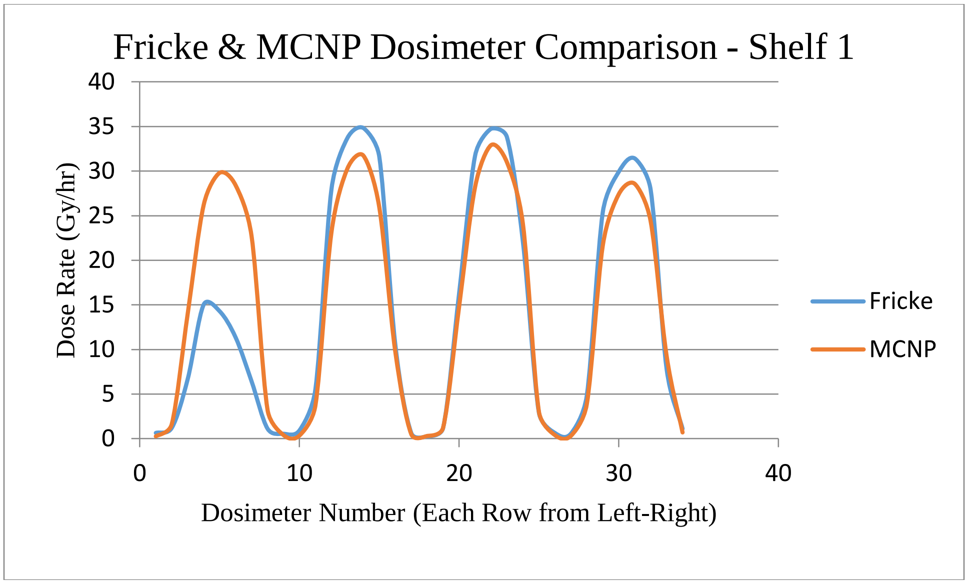

Figure 16: Fricke & MCNP Dosimeters (Rows 1-4) on Shelf 1 (26 cm from Source)
Note the inconsistency in the peak dose rate of Fricke is significantly less than MCNP found in Fricke dosimeters 3-11 on Shelf 1

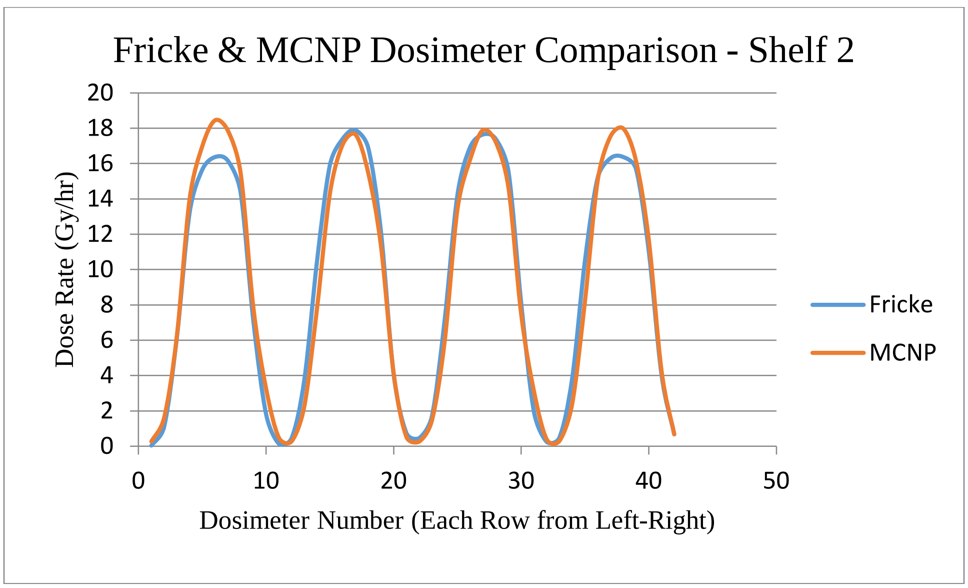

Figure 17: Fricke & MCNP Dosimeters (Rows 1-4) on Shelf 2 (37 cm from Source)

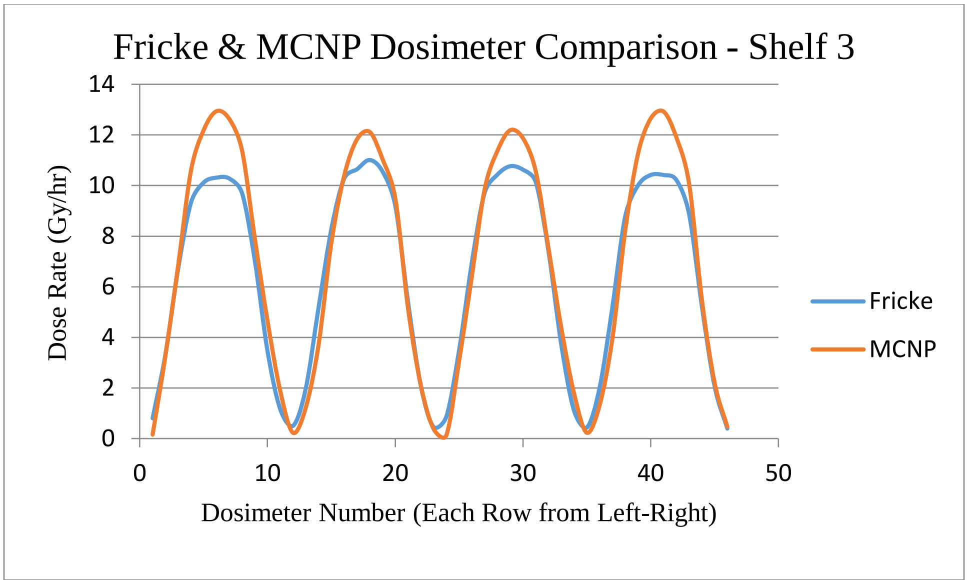

Figure 18: Fricke & MCNP Dosimeters (Rows 1-4) on Shelf 3 (46 cm from Source)

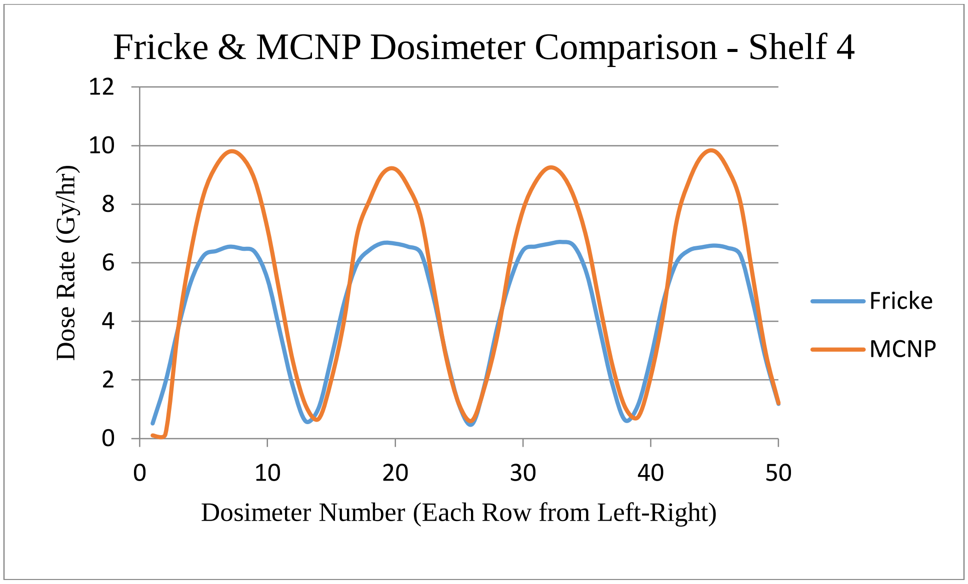

Figure 19: Fricke & MCNP Dosimeters (Rows 1-4) on Shelf 1 (53.75 cm from Source)

Table 7: Fricke Calculation of Irradiator Activity Using the Average of Dosimeters 19-21; 31-33

Activity Calculation from Dosimeters 19-21; 31-33		
Shelf	**Average Dose Rate (Gy/hr)**	**Calculated Activity (TBq [Ci])**
1	33.41	25.32 [684.38]
2	17.36	26.65 [720.30]
3	10.67	25.31 [683.92]
4	6.63	21.47 [580.18]

Table 8: Z Test Comparison of Fricke and MCNP Results

Z Test Results				
	Shelf 1	**Shelf 2**	**Shelf 3**	**Shelf 4**
Mean Dose Rate	14.84	9.18	6.95	5.54
Variance	157.08	47.39	20.61	10.79
Z (2 tailed)	0.79	0.98	0.57	0.05

CHAPTER 4 - DISCUSSION

The placement of Fricke dosimeter vials based upon the results of the Gafchromic film, and represented in Figure 33, show a significant correlation with one exception. Initially, film results showed a proportional distribution (i.e. no shadowing or a misshapen dose field), therefore dosimeter placement focused on finding the targeted area of exposure horizontally, or east to west shown in the same figure. Exposure in the north to south direction on all shelves appeared normal and determined subsequent Fricke vial placement. The anomaly between film and chemical measures occurred on the first shelf. Dosimeters 3-11 in the first horizontal row shown on Figure 6 produced dose rates that were approximately 50% of the remaining dosimeters on Shelf 1. Gafchromic film irradiation times in Table 2 were checked with resulting Fricke dose rate data to ensure no film was overexposed. Further investigation was attempted by performing a duplicate experiment using separate Fricke solution for all dosimeters on Shelf 1. Measured Fricke dose rates agreed within 10% of the initial experiment shown in Table 5. It is unclear exactly why the inconsistency exists; however, thoughts on a flawed source shape or housing were explored. The repetitive experiment also confirmed the accuracy of the chemical dosimetry. Dose rate anomalies were confined to the first row of dosimeters on Shelf 1. Shelves 2-4 displayed uniform dose rates throughout. It was assumed that the trajectory of divergent dose rates would not intersect subsequent shelves as the distance from the source was increased and the beam isotropically spread to a greater area, meaning the inconsistency would be off in space in the north direction rather than on Shelves 2-4. For each shelf, dose rate data for the last two dosimeter vials at the edge of the exposure field dropped by approximately 80% or more compared to other more centralized dosimeters.

Four different contoured heat maps were created with Origin software that showed a visual correlation between dose and position on each shelf. Map data in Gy/hr was displayed logarithmically to maintain uniformity between shelves and the exact shelf dimensions maintained on the x and y-axis. Heat maps shown in Figures 6-9 are very similar in appearance to the Gafchromic results in Figures 20-23. Therefore, compiled images of Gafchromic film were overlaid on the Origin heat maps to compare the

Fricke results to the exposed area of the film. The overlay images shown in Figures 28-31 display a strong resemblance and support the Fricke results. In the Origin software, an algorithm extrapolates data from each of the points and calculates data for the rest of the map. One problem that exists with the algorithm is that data is projected to the corners of the shelf, even though no dosimeter data exists in that area. The projection is more pronounced on shelves 1-2, Figures 6 and 7. All heat map deviations to the shelving corners are to areas in which the dose rate would be too low to be useful. Origin heat maps are intended for future irradiator use and will be available to operators with specific instructions on software-generated disparities.

Once all physical measurements of the irradiator were taken and dose rate data obtained, MCNP simulations were executed. A few key geometry portions were unknown such as the actual distribution of Cs-137 in the source housing but a consistent distribution was chosen with thin source housing stainless steel encapsulating material. The final code displaying tally data for all 50 dosimeters on Shelf 4 is shown in Figure 32. Each shelf was run independently and a total of 10 million particles simulated. It is well known that increasing the number of particles simulated reduces the error and uncertainties calculated within MCNP but can increase overall runtime. When all simulations are complete, the program generates a text file output with an abundance of useful data. Text file data includes uncertainty, flux through each tally, as well as tally dose per starting particle. By displaying dose rate results per starting particle allows the user to enter an activity level of the source, since each simulation is independent of time in the MCNP program. A modeled activity of 56 TBq was chosen and will be discussed at length later.

Data displayed both in starting particle units, Gy/hr, and uncertainty values are shown in Table 6. Calculated uncertainties for each MCNP tally, or point detector, was extremely low. Of 172 tallies simulated, two simulations produced between 3-6% uncertainty. Five simulations produced just over 1% uncertainty, with the remaining runs less than 1%. Uncertainty is given by the algorithms generated in each particles lifetime until it either reaches a tally, deposits its energy in another material, or is lost (Goorley, 2013). Due to the low significance, MCNP uncertainties are omitted from graphs. MCNP data was converted into the same form as Fricke dosimetry and compared.

Comparison graphs of MCNP versus Fricke dosimetry are shown in Figures 16-19. Each rise and fall of the curve is representative of a row of dosimeters as they are listed in numerical order. It is important to note that the 56 TBq chosen in the MCNP conversion was chosen to closely match Fricke results on Shelf 1. Each subsequent shelf is based on the same activity and a small growing divergence is apparent as distance from the source increases. The anomaly of dose on Shelf 1 is apparent compared to the MCNP model in Figure 12. Even though the peaks of activity gradually deviate the rise and fall of dose is virtually identical on all shelves. The matching characteristics point to a very similar beam width, and inconsistent beam strength toward the center of the shelf. Several methods were utilized to help determine the cause of the difference between Fricke and MCNP values. First, the length source was changed in the MCNP model as well as the thickness of the source housing that did not markedly change the results. Next, thoughts of scattered particles contributing to a higher peak dose rates were explored. Even though the modeled irradiator included the same concrete floor, walls, and ceiling that is physically present, all photon energies below 75 keV were disregarded by the software. In total, photon discrimination changed MCNP dose rates by less than 1%. It is unknown what exact components, either flaws in the irradiator modeling or inconsistencies in a 40-year-old irradiator, would be the cause of contrast between results but more analysis is needed.

In determining further comparison between shelves as well as Fricke and MCNP measurements, the inverse-square law was used. Rather than use a single dosimeter common to each shelf, the average dose rate of a group of dosimeters was used. Throughout shelves 1-4 in both Fricke and MCNP, dosimeters 19-21 and 31-33 remained the most consistent throughout shelving. Six dosimeter points chosen are under the projected collimator region are shown in Figure 33. Each method of measurement was plotted separately with a trend line fit to the average of six dosimeters on shelves 1-4. Statistical fit or R^2 values were 0.986 for Fricke and 0.987 for MCNP, shown in Figures 10 and 11. A graphical exponent of $x^{-2.18}$ was calculated for Fricke, which is close to the desired x^{-2} of the inverse square law. The MCNP graph contained an exponent value of $x^{-1.65}$, further away from the desired x^{-2} of the inverse square law. Each measured point was at a distance far enough for the cylindrical Cs-137 source inside the irradiator to be considered a point source. MCNP modeling in theory should be perfect within the principles of the inverse square law and thus suggests that more investigation is needed into the model.

Perhaps the largest surprise in investigating J.L Shepherd irradiator dose rates was the calculated activity. Recall that the source is not NIST traceable and the only indication of activity was on an affixed label plate from 1976. Referring to Table 1, the calculated activity was 90.16 TBq. Following along the same guidelines as the inverse square law, the average of the same six dosimeters was used to calculate the expected activity. Using the point source equation with a specific gamma ray constant associated with Cs-137 of 0.33 R-m^2/Ci-hr (Johnson, 2016) and rearranging to solve for the source activity, values calculated are shown in Table 7. It is extremely unlikely that the source housing could shield enough photons to impact the activity calculation by such magnitude. Since the rate of decay of Cs-137 is changeless, thoughts of a under loaded source arise. It is impossible to know if the 222 TBq [6000 Ci] J.L. Shepherd advertises is accurate, or if creation of the Cs-137 source was contracted to a company which did not load the appropriate activity. Another possibility is that the source is not deploying completely into the irradiation port, and is partly shielded. The degree of likeliness that a part of the source was removed or leaked out is zero, due to proper survey documentation as well as the age of the facility.

Given the range of Fricke dosimetry between 20-400 Gy, circumstances arose which resulted in the under exposure of dosimeters at the edge of the exposure field. If the required dose is met for these dosimeters to within the proven primary standard accuracy of Fricke, then those in the primary radiation field would have been overexposed. In most situations, the underexposed dosimeters read 25-30% compared to the closest preceding one. Considering the fact that data remained consistent throughout the different rows, it is sufficient to say that these dose rates are comparable.

When selecting a material to contain the Fricke solution, plastic was chosen over glass for its lower density and low attenuation of photons. Both the cap and walls of each scintillation vial were measured with a dial caliper. The plastic material used was nearly transparent to photons, as calculated using the change in intensity proportion with the natural logarithm of the attenuation coefficient and thickness of absorber, in this case plastic or glass. By using an energy attenuation coefficient of polyethylene (μ_{en}/p) value of 0.03375 cm^2g^{-1} of a 0.6 MeV gamma, accounting for the plastic density of 0.86 gcm^3, and using a measured thickness of the scintillation vial at 0.126 cm, the overall dose is affected by less than 1% (Johnson, 2012).

Finally, proving that the results of Fricke and MCNP were independent led to separate two-tailed Z tests of both data sets on each shelf. Displayed in Table 8, the comparison lists a difference in means, proving that each method can be relied upon to make a decision on whether or not the facility could be calibrated. In total, the methods used including repetitive Fricke experiments, inverse square law calculation, and overall comparison to MCNP proved suitable to validate the Fricke dosimeter values as definitive for future irradiator use, with some consideration on repetitive use. MCNP modeling for aging irradiators or those with unknown internal geometries, source distribution, and NIST traceable activities should be carefully contemplated. Fricke dosimetry was proven extremely successful for the purposes of calibration and could be relied upon given few factors. If the chemical dosimetry system is to be solely relied upon, then a portion of the mixture should be irradiated to known dose and measured to confirm accuracy. Otherwise, a separate dosimetry measuring method should be used. Comparison to MCNP software was instrumental in proving inconsistencies between an ideal model compared to actual results. MCNP's use for calibration purposes would be more influential the closer the created model is to the actual irradiator in both shape and selection of proper constructed material.

CHAPTER 5 –CONCLUSION

Calibration of CSU’s J.L. Shepherd irradiator with Fricke dosimetry and MCNP software uncovered important disparities previously unknown to operators. Gafchromic film used to ascertain dose rates was useful in the placement of Fricke dosimetry, which showed a non-homogeneous dose distribution on the north side of the first shelf. Physical measurements and one internal schematic of the irradiator used to generate a model of the irradiator showed an initial match within 10% of Fricke on the first two shelving positions. As distance increased from the irradiator source, results from Fricke and MCNP diverged in the peak dose measured. Centralized Fricke dosimeters averaged from all four shelves proved that the irradiators listed activity was incorrect or the source was only partially deployed into the exposure port. Based upon the methods used, accuracy of Fricke dosimetry, and matching characteristics of Fricke with Gafchromic film and MCNP, the results obtained can be considered accurate for future irradiator use. With respect to future calibrations, particular attention should be given to the irradiator age, design, and source geometry as actual results compared to an ideal model generated with MCNP may prove difficult to acquiesce.

REFERENCES

Al-Mughrabi, M., & Neubauer, J. (2007). Identification of radioactive sources and devices: reference manual. Vienna: International Atomic Energy Agency.

ASTM Standard 51026 E, 2015, “Standard Practice for Using the Fricke Dosimetry System,” ASTM International, West Conshohocken, PA, 2003

Attix, F. H., Roesch, W. C., & Tochilin, E. (1966). Radiation dosimetry (Vol. 2, Instrumentation). New York: Academic Press.

Cheung, T., Butson, M. J., & Yu, P. K. (2005). Post-irradiation colouration of Gafchromic EBT radiochromic film. Physics in Medicine and Biology, 50(20).

Efficient Protocols for Accurate Radiochromic Film Calibration and Dosimetry . (2016). Covington, KY: Ashland Inc. Retrieved from http://www.gafchromic.com/documents/Efficient%20Protocols%20for%20Calibration%20and%20Dosimetry.pdf

GafChromic® EBT2 and EBT3 Films for Ball Cube II Phantom. (2014). Covington, KY: Ashland Inc. Retrieved from http://www.gafchromic.com/documents/BallCube_II_EBT2_3_box_insert_201404.pdf

Goorley, J et. al. (2013). Initial MCNP6 Release Overview - MCNP6 version 1.0. Los Alamos, NM: LANL. Retreived from https://laws.lanl.gov/vhosts/mcnp.lanl.gov/pdf_files/la-ur-13-22934.pdf

Irradiators [Radiation Safety Division]. (2016). Beltsville, MD: USDA. Retrieved from https://www.dm.usda.gov/ohsec/rsd/irradiators.htm#pt1.

Johnson, T. (2016). Introduction to health physics. New York City, NY: Mcgraw-Hill Education.

Johnson, T. E., Birky, B. K., & Shleien, B. (2012). Health physics and radiological health. Philadelphia: Wolters Kluwer Health/Lippincott Williams & Wilkins.

Minniti, R., & Seltzer, S. (2007). Calibration of a 137Cs γ-ray beam irradiator using large size chambers. Applied Radiation and Isotopes, 65(4), 401-406.

Podgorsak, E. D. (2005). Radiation oncology physics: a handbook for teachers and students. Vienna: International Atomic Energy Agency.

Radiation Control Manual. (2016). Fort Collins, CO: Colorado State University Radiation Control Office. Retrieved from http://www.ehs.colostate.edu/DV2.aspx?ID=176

Sohrabpour, M., Hassanzadeh, M., Shahriari, M., & Sharifzadeh, M. (2002a). Gamma irradiator dose mapping simulation using the MCNP code and benchmarking with dosimetry. Applied Radiation and Isotopes, 57(4), 537-542.

Sohrabpour, M., Hassanzadeh, M., Shahriari, M., & Sharifzadeh, M. (2002b). Dose distribution of the IR-136 irradiator using a Monte Carlo code and comparison with dosimetry. Radiation Physics and Chemistry, 63(3-6), 769-772.

Vandana, S., Shaiju, V., Sharma, S., Mhatre, S., Shinde, S., Chourasiya, G., & Mayya, Y. (2011). Dosimetry of gamma chamber blood irradiator using Gafchromic EBT film. Applied Radiation and Isotopes, 69(1), 130-135.

Wang, W., Matthews, K. L., & Teague, R. E. (2008). Dose Rates from a Cobalt-60 Pool Irradiator Measured with Fricke Dosimeters. Health Physics, 94 (Suppl 2).

APPENDIX A

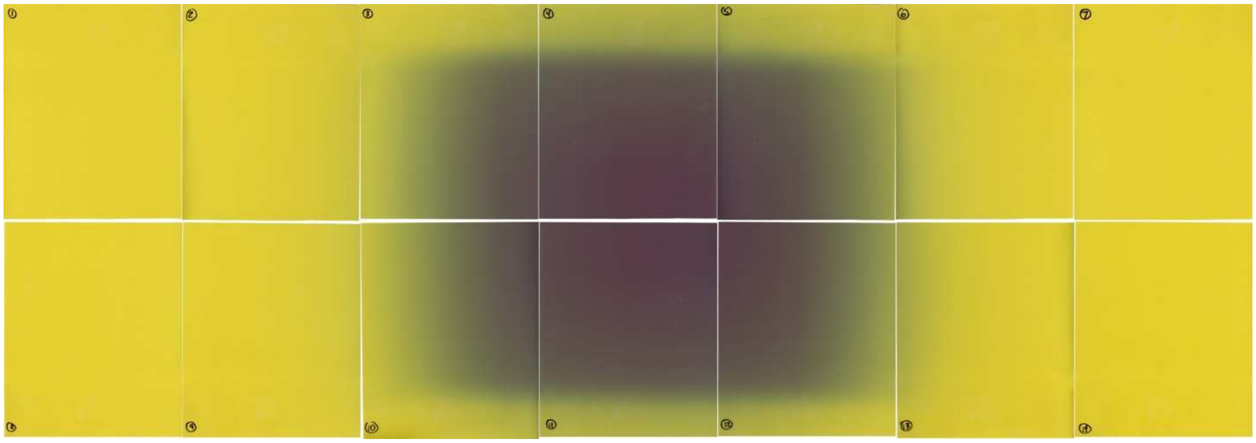

Figure 20: Gafchromic Film Results Shelf Position 1

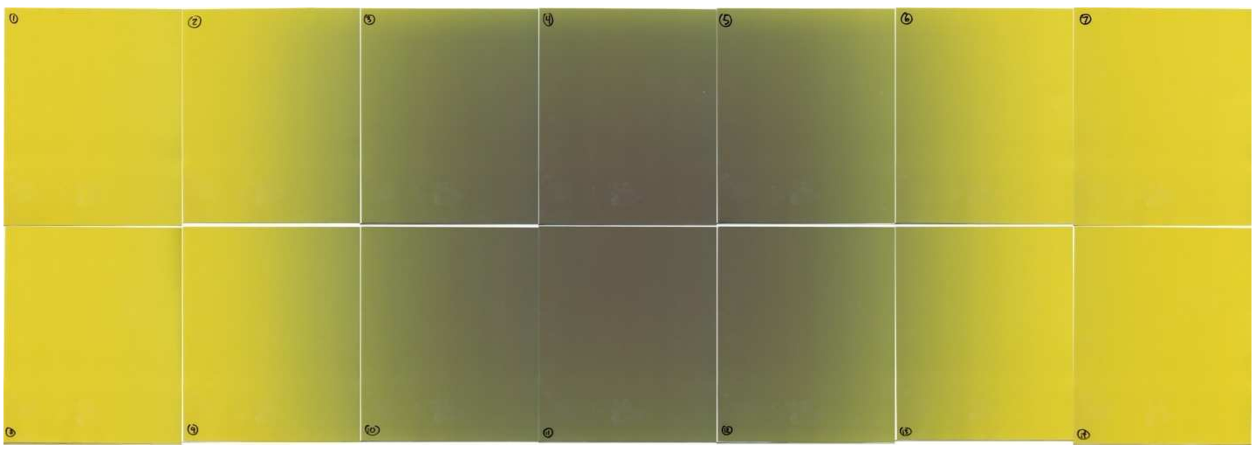

Figure 21: Gafchromic Film Results Shelf Position 2

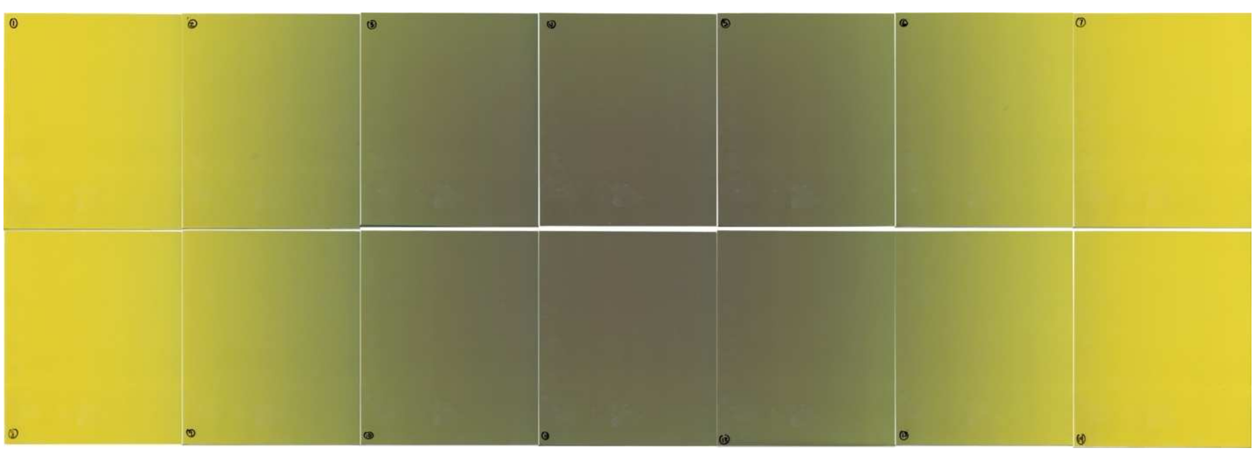

Figure 22: Gafchromic Film Results Shelf Position 3

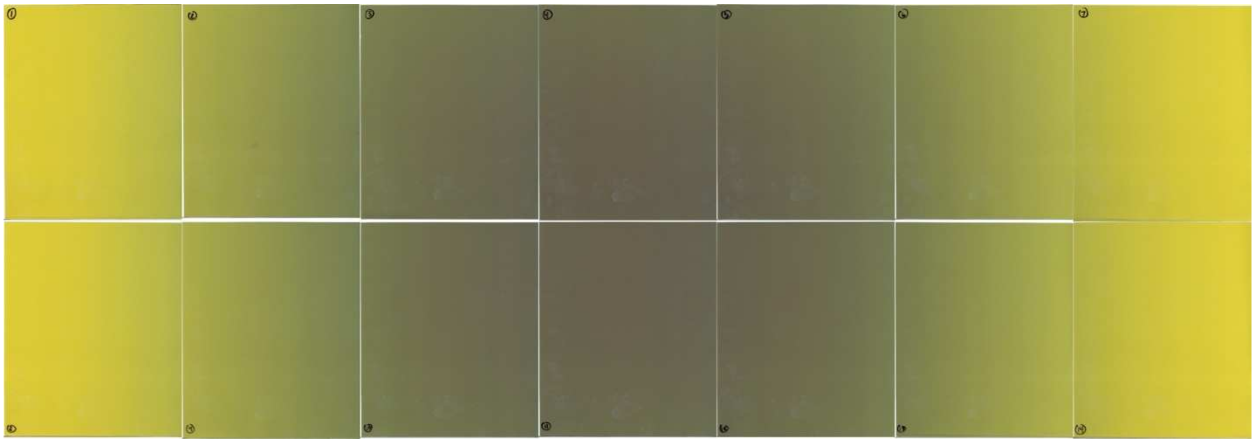

Figure 23: Gafchromic Film Results Shelf Position 4

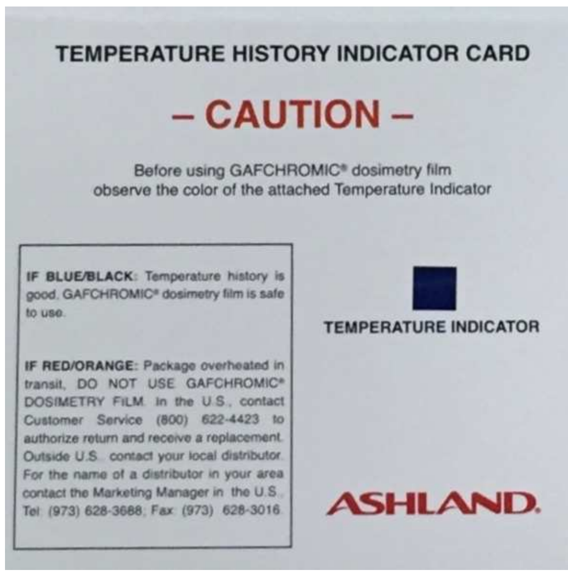

Figure 24: Gafchromic Temperature History Indicator Card

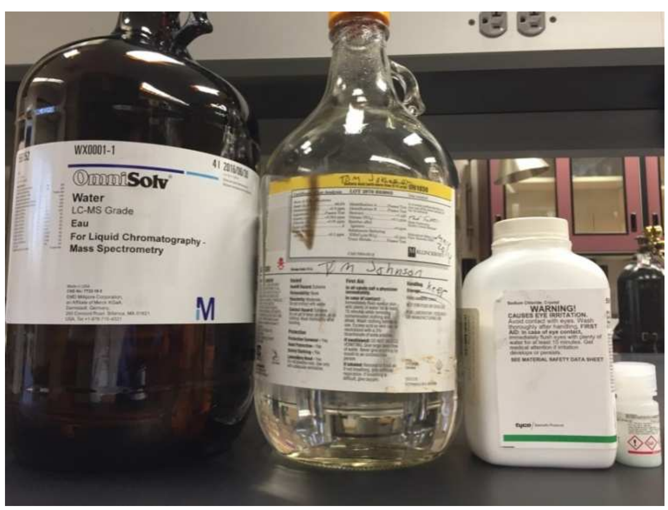

Figure 25: Chemicals Used to Mix Fricke (from left to right): LCMS Water, Sulfuric Acid, Sodium Chloride, and Ferrous Ammonium Sulfate

Figure 26: Wheaton Scientific Liquid Scintillation Vials

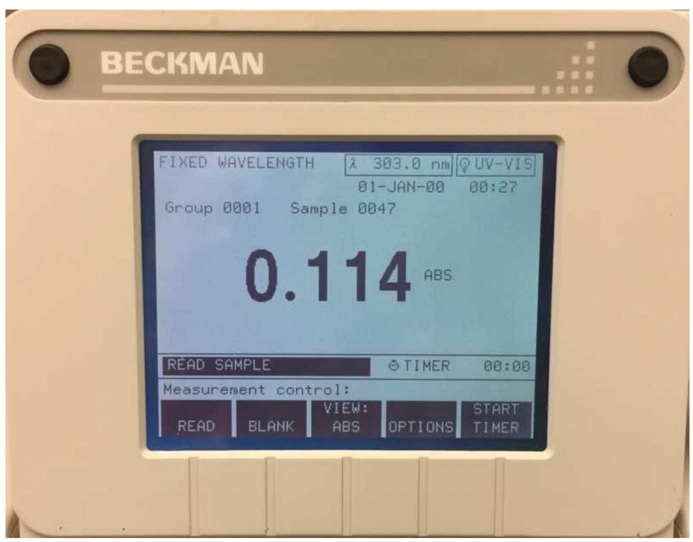

Figure 27: Beckman DU 530 Spectrophotometer

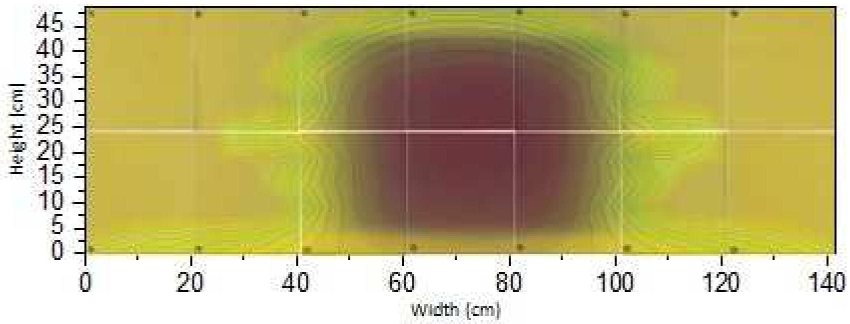

Figure 28: Overlay of Gafchromic Film Over Origin Heat Map Shelf 1

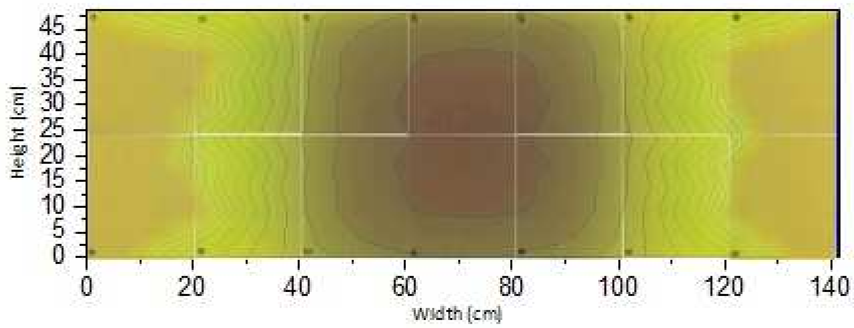

Figure 29: Overlay of Gafchromic Film Over Origin Heat Map Shelf 2

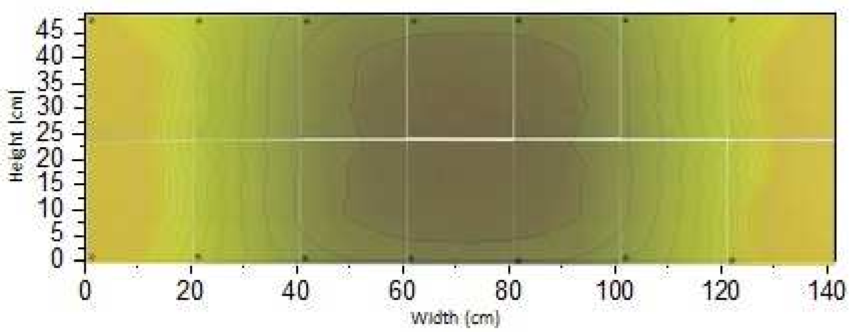

Figure 30: Overlay of Gafchromic Film Over Origin Heat Map Shelf 3

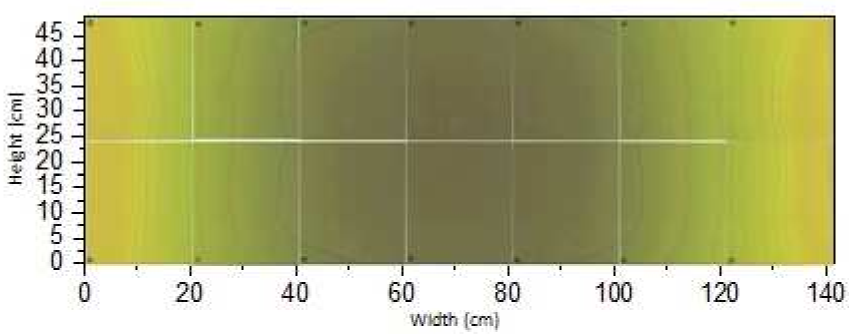

Figure 31: Overlay of Gafchromic Film Over Origin Heat Map Shelf 4

```
J.L. Shepherd 81-14 MCNP Model
c    ***************************************************************************
c    CELLS
c    ***************************************************************************
c
1 5 -2.6989 -1 -2 -3 -4 5 -6 $ALUMINUM STACK
2 3 -1.2048e-3 -7 -8 -9 -10 -11 5 12 -13 14 -15 (1:2:3:4:-5:6) $AIR AROUND ALUMINUM
STACK
3 5 -2.6989 12 -13 14 -15 16 -5 $ALUMINUM PLATE
4 1 -11.3 (7:8:9:10:11:-5) 12 -13 14 -15 5 -11 $LEAD BOX
5 1 -11.3 ((-12:13:-14:15:11:-5) -17 18 -19 (20:-18:21)):&
          (-28 29 -18 (20:-30:18)) $LEAD CYLINDER OUTSIDE OF BOX
6 3 -1.2048E-3 -20 30 -21 (-12:13:-14:15:11:-5) (22:-23:24) $AIR HOUSING
7 6 -7.874 -22 23 -24 (25:-26:27) $STEEL HOUSING
8 8 -2.93 -25 26 -27 $SOURCE SPOT
9 4 -8 (31 -32 33 -34 35 -36):(31 -32 37 -38 35 -36):(39 -40 33 -34 35 -36):&
       (39 -40 37 -38 35 -36) $ALL OF THE STEEL SUPPORTS
10 7 -0.64 41 -42 43 -44 45 -46 $MOVABLE SHELF
11 2 -2.3 ((47 -48 49 -50 35 -51):(-52:48:-53:54:-35:51)) 55 -56 57 -58 59 -60
$CONCRETE PILLAR AND WALLS
12 3 -1.2048E-3 (-12:13:-14:15:-5:11) (-12:13:-14:15:-16:5) (17:-18:19) &
               (28:-29:18) (-31:32:-33:34:-35:36) (-31:32:-37:38:-35:36) &
               (-39:40:-33:34:-35:36) (-39:40:-37:38:-35:36) &
               (-41:42:-43:44:-45:46) (-47:48:-49:50:-35:51) &
               52 -48 53 -54 35 -51 $AIR INSIDE THE ROOM
13 0 (-55:56:-57:58:-59:60) $REST OF SPACE

c    ***************************************************************************
c    SURFACES
c    ***************************************************************************
c
c ------------------------------------------------------------------------------
c ALUMINUM STACK
1 P 14.605 -2.24 141.288 34.675 -2.24 141.288 38.12 -5.665 140.335 $Aluminum 1
2 P 34.675 -2.24 141.288 38.12 -5.665 140.335 34.675 2.24 141.288  $Aluminum 2
3 P 34.675 2.24 141.288 14.605 2.24 141.288 11.43 5.665 140.335    $Aluminum 3
4 P 14.605 -2.24 141.288 14.605 2.24 141.288 11.43 5.665 140.335   $Aluminum 4
5 PZ 140.355 $Bottom of Aluminum
6 PZ 141.288 $Top of Aluminum
c ------------------------------------------------------------------------------
c "SLANTED PLANES"
7 P 15.0813 4.7625 155.575 34.4488 4.7625 155.575 38.735 12.7 140.335
8 P 15.0813 -4.7625 155.575 34.4488 -4.7625 155.575 38.735 -12.7 140.335
9 P 34.4488 4.7625 155.575 34.4488 -4.7625 155.575 38.735 -12.7 140.335
10 P 15.0813 4.7625 155.575 15.0813 -4.7625 155.575 10.785 12.7 140.335
11 PZ 155.575 $Top
c BOTTOM IS SURFACE 5, SAME AS ALUMINUM STACK
c ------------------------------------------------------------------------------
c ALUMINUM PLATE
12 PX 10.795
13 PX 38.735
14 PY -12.7
15 PY 12.7
16 PZ 140.176
c TOP IS SURFACE 5, SAME AS ALUMINUM STACK
c ------------------------------------------------------------------------------
c BOX AROUND ALUMINUM AND JUNK
c SAME X AND Y DIMENSIONS AS ALUMINUM PLATE, SURFACES 12-15
c BOTTOM IS TOP OF ALUMINUM PLATE, SURFACE 5
c TOP IS TOP OF ALUMINUM STACK, SURFACE 11
c ------------------------------------------------------------------------------
c BIG LEAD CYLINDER
17 C/X 0 158.75 17.78
```

```
18 PX 0     $Left Edge
19 PX 80.01 $Right Edge
c -------------------------------------------------------------------------------
C SMALL CYLINDER IN LEAD FOR SOURCE HOUSING
20 C/X 0 158.75 5.71
30 PX -85.09 $Left Edge
21 PX 69.85  $Right Edge
c -------------------------------------------------------------------------------
C STEEL SOURCE HOUSING
22 C/X 0 158.75 2.38125
23 PX 16.8275 $Left Edge
24 PX 32.7025 $Right Edge
c -------------------------------------------------------------------------------
C INNER CYLINDER IN STEEL HOUSING
25 C/X 0 158.75 2.06375
26 PX 17.145 $Left Edge
27 PX 32.385 $Right Edge
c -------------------------------------------------------------------------------
C SMALLER LEAD CYLINDER
28 C/X 0 158.75 11.43
29 PX -90.17 $Left Edge
C RIGHT EDGE IS SAME AS LEFT EDGE OF BIG CYLINDER, SURFACE 18
c -------------------------------------------------------------------------------
C FORWARD LEFT STEEL SUPPORT
31 PX -51.435
32 PX -36.195
33 PY -41.275
34 PY -26.035
35 PZ 0
36 PZ 192.405
c -------------------------------------------------------------------------------
C REAR LEFT STEEL SUPPORT
C SURFACE 31
C SURFACE 32
37 PY 24.765
38 PY 40.005
C SURFACE 35
C SURFACE 36
c -------------------------------------------------------------------------------
C FORWARD RIGHT STEEL SUPPORT
39 PX 84.455
40 PX 99.695
C SURFACE 33
C SURFACE 34
C SURFACE 35
C SURFACE 36
c -------------------------------------------------------------------------------
C REAR RIGHT STEEL SUPPORT
C SURFACE 39
C SURFACE 40
C SURFACE 37
C SURFACE 38
C SURFACE 35
C SURFACE 36
c -------------------------------------------------------------------------------
C MOVABLE SHELF
41 PX -48.26
42 PX 93.345
43 PY -25.0825
44 PY 23.8125
45 PZ 124.906
46 PZ 126.176
c -------------------------------------------------------------------------------
```

```
C CONCRETE PILLAR
47 PX 208.28
48 PX 254
49 PY -43.815
50 PY 8.255
C SURFACE 35
51 PZ 328.295
c ---------------------------------------------------------------------------
C INNER WALL OF ROOM
52 PX -146.685
C SURFACE 48
53 PY -229.235
54 PY 79.375
C SURFACE 35
C SURFACE 51
c ---------------------------------------------------------------------------
C OUTER PLANES THAT MAKE WALL OF THE ROOM.
55 PX -246.685
56 PX 354
57 PY -329.235
58 PY 179.375
59 PZ -100
60 PZ 428.295

c    **************************************************************************
c    DATA
c    **************************************************************************
c
c ---------------------------------------------------------------------------
C IMPORTANCES
imp:p 1 12r
c ---------------------------------------------------------------------------
C MATERIALS
m1 82000 -1                                                  $lead 11.3
m2 1001 0.1170 8016 0.6082 14000 0.2748                      $concrete 2.3
m3 7014 -0.7553 8016 -0.2318 18000 -0.01282 6012 -0.000125   $air 1.2048e-3
m4 6000 -0.002 25000 -0.007 26000 -0.991                     $steel 8.0
m5 13000 -1.000000                                           $aluminum 2.6989
m6 6000 -0.002000 14000 -0.004000 15000 -0.000300 16000 -0.000200 23000 &
   -0.003000 24000 -0.115000 25000 -0.006000 26000 -0.849500 28000 -0.005000 &
   42000 -0.010000 74000 -0.005000                           $stainless 7.874
m7 1001 -0.059642 6000 -0.497018 7000 -0.004970 8000 -0.427435 12000 &
   -0.001988 16000 -0.004970 19000 -0.001988 20000 -0.001988 $wood 0.64
m8 55137 -0.4064 56137 -0.5936                               $Source material
c ---------------------------------------------------------------------------
C SOURCE
SDEF pos=17.146 0 158.75 axs=1 0 0 rad=d1 ext=d2 erg=0.6617 PAR=2
si1 0 2.06275
sp1 -21 1
si2 0 15.238
sp2 -21 0
c ---------------------------------------------------------------------------
C TALLY HO!
c ---------------------------------------------------------------------------
C ROW 1
F5:P -38.1454 15.875 126.946 0.75
DE5 0.01 0.015 0.02 0.03 0.04 0.05 0.06 0.08 0.1 0.150 0.2 0.3 0.4 0.5 0.6 &
     0.8
DF5 7.43 3.12 1.68 0.721 0.429 0.323 0.289 0.307 0.371 0.599 0.856 1.380 &
     1.890 2.38 2.84 3.69
F15:P -28.0307 15.875 115.561 0.75
DE15 0.01 0.015 0.02 0.03 0.04 0.05 0.06 0.08 0.1 0.150 0.2 0.3 0.4 0.5 0.6 &
     0.8
```

```
DF15 7.43 3.12 1.68 0.721 0.429 0.323 0.289 0.307 0.371 0.599 0.856 1.380 &
     1.890 2.38 2.84 3.69
F25:P -17.9161 15.875 115.561 0.75
DE25 0.01 0.015 0.02 0.03 0.04 0.05 0.06 0.08 0.1 0.150 0.2 0.3 0.4 0.5 0.6 &
     0.8
DF25 7.43 3.12 1.68 0.721 0.429 0.323 0.289 0.307 0.371 0.599 0.856 1.380 &
     1.890 2.38 2.84 3.69
F35:P -7.80143 15.875 115.561 0.75
DE35 0.01 0.015 0.02 0.03 0.04 0.05 0.06 0.08 0.1 0.150 0.2 0.3 0.4 0.5 0.6 &
     0.8
DF35 7.43 3.12 1.68 0.721 0.429 0.323 0.289 0.307 0.371 0.599 0.856 1.380 &
     1.890 2.38 2.84 3.69
F45:P 2.31321 15.875 115.561 0.75
DE45 0.01 0.015 0.02 0.03 0.04 0.05 0.06 0.08 0.1 0.150 0.2 0.3 0.4 0.5 0.6 &
     0.8
DF45 7.43 3.12 1.68 0.721 0.429 0.323 0.289 0.307 0.371 0.599 0.856 1.380 &
     1.890 2.38 2.84 3.69
F55:P 12.4279 15.875 115.561 0.75
DE55 0.01 0.015 0.02 0.03 0.04 0.05 0.06 0.08 0.1 0.150 0.2 0.3 0.4 0.5 0.6 &
     0.8
DF55 7.43 3.12 1.68 0.721 0.429 0.323 0.289 0.307 0.371 0.599 0.856 1.380 &
     1.890 2.38 2.84 3.69
F65:P 22.5425 15.875 115.561 0.75
DE65 0.01 0.015 0.02 0.03 0.04 0.05 0.06 0.08 0.1 0.150 0.2 0.3 0.4 0.5 0.6 &
     0.8
DF65 7.43 3.12 1.68 0.721 0.429 0.323 0.289 0.307 0.371 0.599 0.856 1.380 &
     1.890 2.38 2.84 3.69
F75:P 32.6571 15.875 115.561 0.75
DE75 0.01 0.015 0.02 0.03 0.04 0.05 0.06 0.08 0.1 0.150 0.2 0.3 0.4 0.5 0.6 &
     0.8
DF75 7.43 3.12 1.68 0.721 0.429 0.323 0.289 0.307 0.371 0.599 0.856 1.380 &
     1.890 2.38 2.84 3.69
F85:P 42.7718 15.875 115.561 0.75
DE85 0.01 0.015 0.02 0.03 0.04 0.05 0.06 0.08 0.1 0.150 0.2 0.3 0.4 0.5 0.6 &
     0.8
DF85 7.43 3.12 1.68 0.721 0.429 0.323 0.289 0.307 0.371 0.599 0.856 1.380 &
     1.890 2.38 2.84 3.69
F95:P 54.8864 15.875 115.561 0.75
DE95 0.01 0.015 0.02 0.03 0.04 0.05 0.06 0.08 0.1 0.150 0.2 0.3 0.4 0.5 0.6 &
     0.8
DF95 7.43 3.12 1.68 0.721 0.429 0.323 0.289 0.307 0.371 0.599 0.856 1.380 &
     1.890 2.38 2.84 3.69
F105:P 63.0011 15.875 115.561 0.75
DE105 0.01 0.015 0.02 0.03 0.04 0.05 0.06 0.08 0.1 0.150 0.2 0.3 0.4 0.5 0.6 &
     0.8
DF105 7.43 3.12 1.68 0.721 0.429 0.323 0.289 0.307 0.371 0.599 0.856 1.380 &
     1.890 2.38 2.84 3.69
F115:P 73.1157 15.875 115.561 0.75
DE115 0.01 0.015 0.02 0.03 0.04 0.05 0.06 0.08 0.1 0.150 0.2 0.3 0.4 0.5 0.6 &
     0.8
DF115 7.43 3.12 1.68 0.721 0.429 0.323 0.289 0.307 0.371 0.599 0.856 1.380 &
     1.890 2.38 2.84 3.69
F125:P 83.2304 15.875 115.561 0.75
DE125 0.01 0.015 0.02 0.03 0.04 0.05 0.06 0.08 0.1 0.150 0.2 0.3 0.4 0.5 0.6 &
     0.8
DF125 7.43 3.12 1.68 0.721 0.429 0.323 0.289 0.307 0.371 0.599 0.856 1.380 &
     1.890 2.38 2.84 3.69
c --------------------------------------------------------------------------------
C ROW 2
F135:P -37.3673 5.175 115.561 0.75
DE135 0.01 0.015 0.02 0.03 0.04 0.05 0.06 0.08 0.1 0.150 0.2 0.3 0.4 0.5 0.6 &
     0.8
DF135 7.43 3.12 1.68 0.721 0.429 0.323 0.289 0.307 0.371 0.599 0.856 1.380 &
```

```
     1.890 2.38 2.84 3.69
F145:P -26.4746 5.175 115.561 0.75
DE145 0.01 0.015 0.02 0.03 0.04 0.05 0.06 0.08 0.1 0.150 0.2 0.3 0.4 0.5 0.6 &
     0.8
DF145 7.43 3.12 1.68 0.721 0.429 0.323 0.289 0.307 0.371 0.599 0.856 1.380 &
     1.890 2.38 2.84 3.69
F155:P -15.5819 5.175 115.561 0.75
DE155 0.01 0.015 0.02 0.03 0.04 0.05 0.06 0.08 0.1 0.150 0.2 0.3 0.4 0.5 0.6 &
     0.8
DF155 7.43 3.12 1.68 0.721 0.429 0.323 0.289 0.307 0.371 0.599 0.856 1.380 &
     1.890 2.38 2.84 3.69
F165:P -4.68923 5.175 115.561 0.75
DE165 0.01 0.015 0.02 0.03 0.04 0.05 0.06 0.08 0.1 0.150 0.2 0.3 0.4 0.5 0.6 &
     0.8
DF165 7.43 3.12 1.68 0.721 0.429 0.323 0.289 0.307 0.371 0.599 0.856 1.380 &
     1.890 2.38 2.84 3.69
F175:P 6.20346 5.175 115.561 0.75
DE175 0.01 0.015 0.02 0.03 0.04 0.05 0.06 0.08 0.1 0.150 0.2 0.3 0.4 0.5 0.6 &
     0.8
DF175 7.43 3.12 1.68 0.721 0.429 0.323 0.289 0.307 0.371 0.599 0.856 1.380 &
     1.890 2.38 2.84 3.69
F185:P 17.0962 5.175 115.561 0.75
DE185 0.01 0.015 0.02 0.03 0.04 0.05 0.06 0.08 0.1 0.150 0.2 0.3 0.4 0.5 0.6 &
     0.8
DF185 7.43 3.12 1.68 0.721 0.429 0.323 0.289 0.307 0.371 0.599 0.856 1.380 &
     1.890 2.38 2.84 3.69
F195:P 27.9888 5.175 115.561 0.75
DE195 0.01 0.015 0.02 0.03 0.04 0.05 0.06 0.08 0.1 0.150 0.2 0.3 0.4 0.5 0.6 &
     0.8
DF195 7.43 3.12 1.68 0.721 0.429 0.323 0.289 0.307 0.371 0.599 0.856 1.380 &
     1.890 2.38 2.84 3.69
F205:P 38.8815 5.175 115.561 0.75
DE205 0.01 0.015 0.02 0.03 0.04 0.05 0.06 0.08 0.1 0.150 0.2 0.3 0.4 0.5 0.6 &
     0.8
DF205 7.43 3.12 1.68 0.721 0.429 0.323 0.289 0.307 0.371 0.599 0.856 1.380 &
     1.890 2.38 2.84 3.69
F215:P 49.7742 5.175 115.561 0.75
DE215 0.01 0.015 0.02 0.03 0.04 0.05 0.06 0.08 0.1 0.150 0.2 0.3 0.4 0.5 0.6 &
     0.8
DF215 7.43 3.12 1.68 0.721 0.429 0.323 0.289 0.307 0.371 0.599 0.856 1.380 &
     1.890 2.38 2.84 3.69
F225:P 60.6669 5.175 115.561 0.75
DE225 0.01 0.015 0.02 0.03 0.04 0.05 0.06 0.08 0.1 0.150 0.2 0.3 0.4 0.5 0.6 &
     0.8
DF225 7.43 3.12 1.68 0.721 0.429 0.323 0.289 0.307 0.371 0.599 0.856 1.380 &
     1.890 2.38 2.84 3.69
F235:P 71.5596 5.175 115.561 0.75
DE235 0.01 0.015 0.02 0.03 0.04 0.05 0.06 0.08 0.1 0.150 0.2 0.3 0.4 0.5 0.6 &
     0.8
DF235 7.43 3.12 1.68 0.721 0.429 0.323 0.289 0.307 0.371 0.599 0.856 1.380 &
     1.890 2.38 2.84 3.69
F245:P 82.4523 5.175 115.561 0.75
DE245 0.01 0.015 0.02 0.03 0.04 0.05 0.06 0.08 0.1 0.150 0.2 0.3 0.4 0.5 0.6 &
     0.8
DF245 7.43 3.12 1.68 0.721 0.429 0.323 0.289 0.307 0.371 0.599 0.856 1.380 &
     1.890 2.38 2.84 3.69
c ----------------------------------------------------------------------------
C ROW 3
F255:P -38.1454 -6.985 115.561 0.75
DE255 0.01 0.015 0.02 0.03 0.04 0.05 0.06 0.08 0.1 0.150 0.2 0.3 0.4 0.5 0.6 &
     0.8
DF255 7.43 3.12 1.68 0.721 0.429 0.323 0.289 0.307 0.371 0.599 0.856 1.380 &
     1.890 2.38 2.84 3.69
```

```
F265:P -28.0307 -6.985 115.561 0.75
DE265 0.01 0.015 0.02 0.03 0.04 0.05 0.06 0.08 0.1 0.150 0.2 0.3 0.4 0.5 0.6 &
     0.8
DF265 7.43 3.12 1.68 0.721 0.429 0.323 0.289 0.307 0.371 0.599 0.856 1.380 &
     1.890 2.38 2.84 3.69
F275:P -17.9161 -6.985 115.561 0.75
DE275 0.01 0.015 0.02 0.03 0.04 0.05 0.06 0.08 0.1 0.150 0.2 0.3 0.4 0.5 0.6 &
     0.8
DF275 7.43 3.12 1.68 0.721 0.429 0.323 0.289 0.307 0.371 0.599 0.856 1.380 &
     1.890 2.38 2.84 3.69
F285:P -7.80143 -6.985 115.561 0.75
DE285 0.01 0.015 0.02 0.03 0.04 0.05 0.06 0.08 0.1 0.150 0.2 0.3 0.4 0.5 0.6 &
     0.8
DF285 7.43 3.12 1.68 0.721 0.429 0.323 0.289 0.307 0.371 0.599 0.856 1.380 &
     1.890 2.38 2.84 3.69
F295:P 2.31321 -6.985 115.561 0.75
DE295 0.01 0.015 0.02 0.03 0.04 0.05 0.06 0.08 0.1 0.150 0.2 0.3 0.4 0.5 0.6 &
     0.8
DF295 7.43 3.12 1.68 0.721 0.429 0.323 0.289 0.307 0.371 0.599 0.856 1.380 &
     1.890 2.38 2.84 3.69
F305:P 12.4279 -6.985 115.561 0.75
DE305 0.01 0.015 0.02 0.03 0.04 0.05 0.06 0.08 0.1 0.150 0.2 0.3 0.4 0.5 0.6 &
     0.8
DF305 7.43 3.12 1.68 0.721 0.429 0.323 0.289 0.307 0.371 0.599 0.856 1.380 &
     1.890 2.38 2.84 3.69
F315:P 22.5425 -6.985 115.561 0.75
DE315 0.01 0.015 0.02 0.03 0.04 0.05 0.06 0.08 0.1 0.150 0.2 0.3 0.4 0.5 0.6 &
     0.8
DF315 7.43 3.12 1.68 0.721 0.429 0.323 0.289 0.307 0.371 0.599 0.856 1.380 &
     1.890 2.38 2.84 3.69
F325:P 32.6571 -6.985 115.561 0.75
DE325 0.01 0.015 0.02 0.03 0.04 0.05 0.06 0.08 0.1 0.150 0.2 0.3 0.4 0.5 0.6 &
     0.8
DF325 7.43 3.12 1.68 0.721 0.429 0.323 0.289 0.307 0.371 0.599 0.856 1.380 &
     1.890 2.38 2.84 3.69
F335:P 42.7718 -6.985 115.561 0.75
DE335 0.01 0.015 0.02 0.03 0.04 0.05 0.06 0.08 0.1 0.150 0.2 0.3 0.4 0.5 0.6 &
     0.8
DF335 7.43 3.12 1.68 0.721 0.429 0.323 0.289 0.307 0.371 0.599 0.856 1.380 &
     1.890 2.38 2.84 3.69
F345:P 54.8864 -6.985 115.561 0.75
DE345 0.01 0.015 0.02 0.03 0.04 0.05 0.06 0.08 0.1 0.150 0.2 0.3 0.4 0.5 0.6 &
     0.8
DF345 7.43 3.12 1.68 0.721 0.429 0.323 0.289 0.307 0.371 0.599 0.856 1.380 &
     1.890 2.38 2.84 3.69
F355:P 63.0011 -6.985 115.561 0.75
DE355 0.01 0.015 0.02 0.03 0.04 0.05 0.06 0.08 0.1 0.150 0.2 0.3 0.4 0.5 0.6 &
     0.8
DF355 7.43 3.12 1.68 0.721 0.429 0.323 0.289 0.307 0.371 0.599 0.856 1.380 &
     1.890 2.38 2.84 3.69
F365:P 73.1157 -6.985 115.561 0.75
DE365 0.01 0.015 0.02 0.03 0.04 0.05 0.06 0.08 0.1 0.150 0.2 0.3 0.4 0.5 0.6 &
     0.8
DF365 7.43 3.12 1.68 0.721 0.429 0.323 0.289 0.307 0.371 0.599 0.856 1.380 &
     1.890 2.38 2.84 3.69
F375:P 83.2304 -6.985 115.561 0.75
DE375 0.01 0.015 0.02 0.03 0.04 0.05 0.06 0.08 0.1 0.150 0.2 0.3 0.4 0.5 0.6 &
     0.8
DF375 7.43 3.12 1.68 0.721 0.429 0.323 0.289 0.307 0.371 0.599 0.856 1.380 &
     1.890 2.38 2.84 3.69
c ---------------------------------------------------------------------------
C ROW 4
F385:P -37.3673 -17.145 115.561 0.75
```

```
DE385 0.01 0.015 0.02 0.03 0.04 0.05 0.06 0.08 0.1 0.150 0.2 0.3 0.4 0.5 0.6 &
     0.8
DF385 7.43 3.12 1.68 0.721 0.429 0.323 0.289 0.307 0.371 0.599 0.856 1.380 &
     1.890 2.38 2.84 3.69
F395:P -26.4746 -17.145 115.561 0.75
DE395 0.01 0.015 0.02 0.03 0.04 0.05 0.06 0.08 0.1 0.150 0.2 0.3 0.4 0.5 0.6 &
     0.8
DF395 7.43 3.12 1.68 0.721 0.429 0.323 0.289 0.307 0.371 0.599 0.856 1.380 &
     1.890 2.38 2.84 3.69
F405:P -15.5819 -17.145 115.561 0.75
DE405 0.01 0.015 0.02 0.03 0.04 0.05 0.06 0.08 0.1 0.150 0.2 0.3 0.4 0.5 0.6 &
     0.8
DF405 7.43 3.12 1.68 0.721 0.429 0.323 0.289 0.307 0.371 0.599 0.856 1.380 &
     1.890 2.38 2.84 3.69
F415:P -4.68923 -17.145 115.561 0.75
DE415 0.01 0.015 0.02 0.03 0.04 0.05 0.06 0.08 0.1 0.150 0.2 0.3 0.4 0.5 0.6 &
     0.8
DF415 7.43 3.12 1.68 0.721 0.429 0.323 0.289 0.307 0.371 0.599 0.856 1.380 &
     1.890 2.38 2.84 3.69
F425:P 6.20346 -17.145 115.561 0.75
DE425 0.01 0.015 0.02 0.03 0.04 0.05 0.06 0.08 0.1 0.150 0.2 0.3 0.4 0.5 0.6 &
     0.8
DF425 7.43 3.12 1.68 0.721 0.429 0.323 0.289 0.307 0.371 0.599 0.856 1.380 &
     1.890 2.38 2.84 3.69
F435:P 17.0962 -17.145 115.561 0.75
DE435 0.01 0.015 0.02 0.03 0.04 0.05 0.06 0.08 0.1 0.150 0.2 0.3 0.4 0.5 0.6 &
     0.8
DF435 7.43 3.12 1.68 0.721 0.429 0.323 0.289 0.307 0.371 0.599 0.856 1.380 &
     1.890 2.38 2.84 3.69
F445:P 27.9888 -17.145 115.561 0.75
DE445 0.01 0.015 0.02 0.03 0.04 0.05 0.06 0.08 0.1 0.150 0.2 0.3 0.4 0.5 0.6 &
     0.8
DF445 7.43 3.12 1.68 0.721 0.429 0.323 0.289 0.307 0.371 0.599 0.856 1.380 &
     1.890 2.38 2.84 3.69
F455:P 38.8815 -17.145 115.561 0.75
DE455 0.01 0.015 0.02 0.03 0.04 0.05 0.06 0.08 0.1 0.150 0.2 0.3 0.4 0.5 0.6 &
     0.8
DF455 7.43 3.12 1.68 0.721 0.429 0.323 0.289 0.307 0.371 0.599 0.856 1.380 &
     1.890 2.38 2.84 3.69
F465:P 49.7742 -17.145 115.561 0.75
DE465 0.01 0.015 0.02 0.03 0.04 0.05 0.06 0.08 0.1 0.150 0.2 0.3 0.4 0.5 0.6 &
     0.8
DF465 7.43 3.12 1.68 0.721 0.429 0.323 0.289 0.307 0.371 0.599 0.856 1.380 &
     1.890 2.38 2.84 3.69
F475:P 60.6669 -17.145 115.561 0.75
DE475 0.01 0.015 0.02 0.03 0.04 0.05 0.06 0.08 0.1 0.150 0.2 0.3 0.4 0.5 0.6 &
     0.8
DF475 7.43 3.12 1.68 0.721 0.429 0.323 0.289 0.307 0.371 0.599 0.856 1.380 &
     1.890 2.38 2.84 3.69
F485:P 71.5596 -17.145 115.561 0.75
DE485 0.01 0.015 0.02 0.03 0.04 0.05 0.06 0.08 0.1 0.150 0.2 0.3 0.4 0.5 0.6 &
     0.8
DF485 7.43 3.12 1.68 0.721 0.429 0.323 0.289 0.307 0.371 0.599 0.856 1.380 &
     1.890 2.38 2.84 3.69
F495:P 82.4523 -17.145 115.561 0.75
DE495 0.01 0.015 0.02 0.03 0.04 0.05 0.06 0.08 0.1 0.150 0.2 0.3 0.4 0.5 0.6 &
     0.8
DF495 7.43 3.12 1.68 0.721 0.429 0.323 0.289 0.307 0.371 0.599 0.856 1.380 &
     1.890 2.38 2.84 3.69
c ----------------------------------------------------------------------------
NPS 1E7
MODE P
```

Figure 32: MCNP Geometry Code from Shelf 4 with all 50 dosimeters

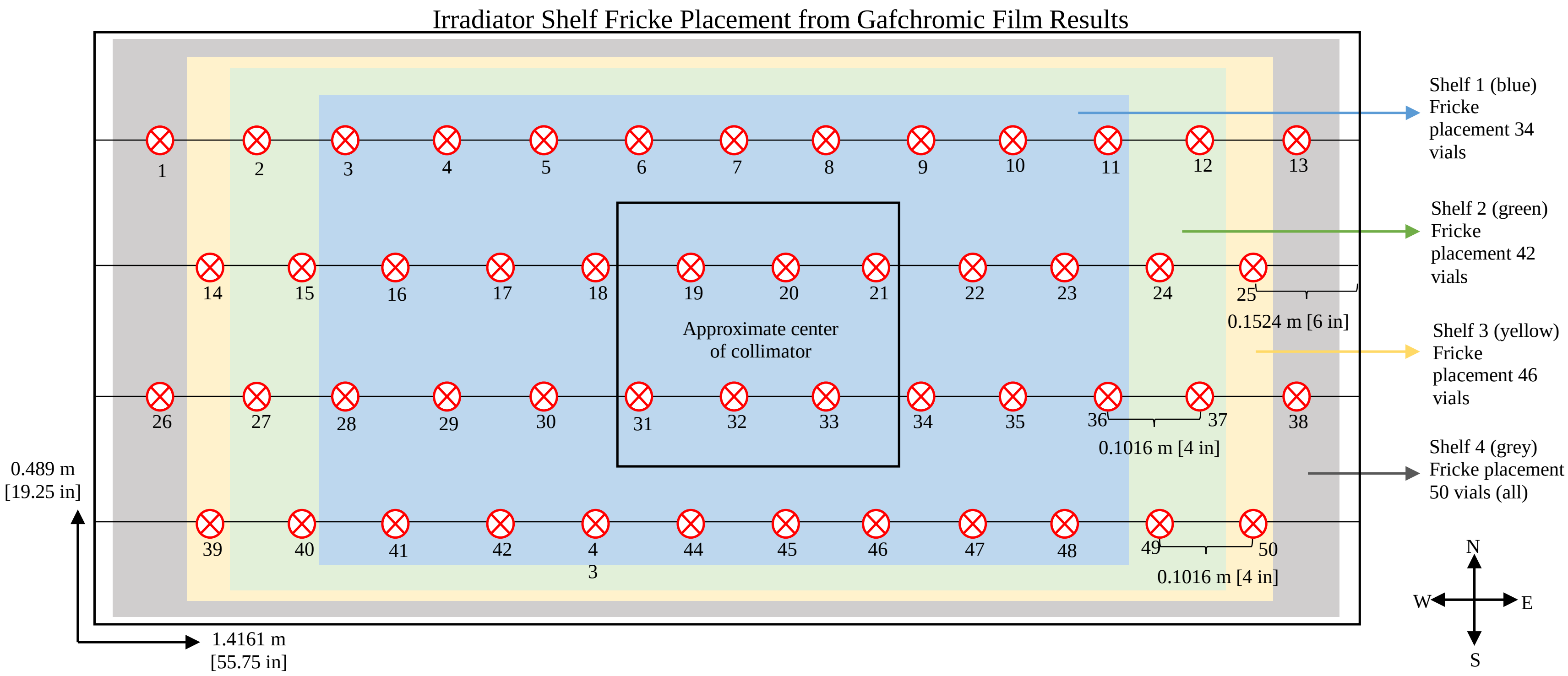

Figure 33: Irradiator Shelf for Fricke Vial placement and MCNP Tally Coordinates